Modern Journal of Statistics
2(2), 129–158
DOI: https://doi.org/10.64389/mjs.2026.02278
https://sphinxsp.org/journal/index.php/mjs

Research article

A New Logarithmic Pie Power-G family of Distributions: Properties and Applications to Medical and Traffic Data

Zubir Shah[1, *], Zubair Ahmad[2], Zahra Almaspoor[2], Faridoon Khan[3], Chrisogonus K. Onyekwere[4], Gadde Srinivasa Rao[5], and Saima K. Khosa[6]

[1]Department of Statistics, Abdul Wali Khan University, Mardan, KP, 23200, Pakistan; zubair_shah@awkum.edu.pk

[2]Department of Statistics, Yazd University, Yazd 8915818411, Iran; z.ferry21@gmail.com; zahra.ferry21@gmail.com

[3]Department of Creative Technologies, FCAI, Air University, Islamabad 44000, Pakistan; faridoon.khan@au.edu.pk

[4]Department of Statistics, Faculty of Physical Sciences, Nnamdi Azikiwe University, P.O. Box 5025, Awka, Nigeria; chrisogonusjohnson@gmail.com

[5]Department of Mathematics and Statistics, University of Dodoma, Dodoma P.O. Box 259, Tanzania; gadde.srinivasa@udom.ac.tz

[6]Department of Mathematics and Statistics, University of Saskatchewan, Saskatoon, SK S7N 5A2, Canada; skk807@mail.usask.ca

***Correspondence:** zubair_shah@awkum.edu.pk.

ARTICLE INFO

Keywords:
New logarithmic Pie Power-G
Inverse Weibull distribution
Statistical properties
Estimation
Simulation study
Real-life Application

Mathematics Subject Classification:
60E05, 60E10, 62G30, 62F10

Important Dates:
Received: 1 April 2026
Revised: 7 June 2026
Accepted: 19 June 2026
Online: 27 June 2026

Copyright © 2026 by the authors. Published under Creative Commons Attribution (CC BY) license.

ABSTRACT

The present study proposes a new versatile family of distributions, called the New Logarithmic Pie Power-G (NLPP-G) family of probability distributions, applying the Power transformation approach. The newly introduced family of distributions has the ability to enhance the flexibility level of the classical distributions without adding extra parameters. A special subcase of the NLPP-G family, by applying the Inverse Weibull model as a baseline member, is suggested. The subcase of the NLPP-G family is called the New Logarithmic Pie Power Inverse Weibull distribution (NLPP-IWD). The cumulative distribution, survival, probability density, and hazard functions of the NLPP-IWD are investigated graphically. Similarly, for the NLPP-IWD, various range of statistical properties, including moments, moment-generating functions, characteristic functions, incomplete moments, mean residual-life, and order statistics, are derived. Based on the Maximum Likelihood Estimation (MLE) method, we have estimated the unknown parameters of the NLPP-IWD, and its practical performance is verified by the Monte Carlo simulation analysis. The numerical results and graphical illustration of the Monte Carlo simulation analysis indicated that biases and mean square error decreased as the sample size increased. Lastly, three are considered to illustrate the practical effectiveness of the NLPP-IWD. The practical performance of the NLPP-IWD is compared with ten well-known distributions using different model selection measures. These evaluations provide empirical evidence that the introduced distribution performs better than ten well-known competing distributions.

1. Introduction

Probability distributions play a significant role in predicting and analyzing real-world phenomena, especially in the realm of applied disciplines, such as reliability engineering, environmental studies, medical sciences, economics, actuarial science, finance, and insurance analysis; further details can be found in Alsadat et al. [1]. Although in the literature on distribution theory, various probability distributions have been proposed and are still growing rapidly. However, no probability distribution has yet been proposed that can handle every phenomenon, particularly the phenomena that have non-monotonic failure rates. Consequently, there is a demand for generalized forms of these existing distributions to capture such phenomena better. This demand has led authors to develop new modifications to existing distributions, incorporating one or more additional parameters to increase their flexibility Almalki and Yuan [2]. Besides, in the literature of distribution theory, many authors have also introduced new methods of developing probability distributions without adding extra parameters to the base members. A review of the literature reveals that many authors have utilized various generators or transformations (i.e., with the support of adding additional parameters or without adding additional parameters) to generate more flexible distributions. In this context, Mudholkar and Srivastava [3] initiated an exponentiated transformation approach of probability distributions, Kumar et al. [4] presented a novel family of distributions by joining a base distribution CDF (cumulative distribution function) with a Sine function, called SS transformation, Maurya et al. [5] suggested a method without adding any additional parameters and named the log transformation family of distributions, Mahdavi and Kundu [6] presented the new alpha power transformation (APT) family of probability distributions which can add one extra parameter to the existing distributions, Elbatal et al. [7] introduced another scheme called a NAPT (new APT) family of probability distributions, Mahmood et al. [8] presented a novel Sine-G family of probability distributions without inserting extra parameters to the baseline distributions, Muhammad et al. [9] introduced a novel method of probability distributions based on a trigonometric function and named as a novel extended cosine-G distributions. Furthermore, Alizadeh et al. [10] suggested the odd logarithmic logistic generated approach of probability distributions for proposing more flexible distributions, whose CDF is

$$F(t;\tau)=1-\frac{\log\left(1-\dfrac{\beta A(t;\tau)^{\alpha}}{A(t;\tau)+\bar{A}(t;\tau)^{\alpha}}\right)}{\log(1-\beta)};\qquad t\in\Re, \tag{1.1}$$

where, $\bar{A}(t;\tau)$ is the survival function (i.e., $\bar{A}(t;\tau)=1-A(t;\tau)$) of any base distribution with parameter vector τ and $\alpha>0$, and $0<\beta<1$. Similarly, Lone and Jan [11] defined the new Pie-exponentiated method for constructing flexible distributions, whose CDF is

$$F(t;\tau)=\frac{\pi^{\{A(t;\tau)\}^{\alpha}}-1}{\pi-1};\qquad \alpha>0, t\in\Re, \tag{1.2}$$

where, $A(t;\tau)$ is the CDF of the base member with parameter vector τ. Also using the transformation method, Ahmad et al. [12] introduced a new cosine generator method with application to the Weibull distribution, whose CDF is

$$F(t;\tau)=1-\cos\left(\frac{\pi\left(2-2^{\bar{A}(t;\tau)}\right)}{2}\right);\qquad t\in\Re, \tag{1.3}$$

where, $\bar{A}(t;\tau)=1-A(t;\tau)$ and τ is the parameter vector of the base member. Recently, Sapkota et al. [13] introduced the SPPO-G (Sine Pie Power odd-G) method of probability distributions, incorporating the Sine-function and pie power odd ratio, whose CDF is

$$F(t;\tau)=\sin\left(\frac{\pi}{2}\left(1-\pi^{-\left(\frac{A(t;\tau)}{1-A(t;\tau)}\right)}\right)\right);\qquad t\in\Re, \tag{1.4}$$

where, $A(t;\tau)$ is the CDF of any baseline probability distribution with parameter vector τ. Using the Sine π-power odd-G approach, Sapkota et al. [13] also enhanced the elasticity power of the Weibull distribution. For further details on developing probabilistic models that utilize the logarithmic and transformation methods, refer to Kavya and Manoharan [14], Lone et al. [15], Elgarhy et al. [16], and Bashiru et al. [17].

Motivated by the above comprehensive argument, in the present paper, we also present a novel method to increase the versatility of existing models, based on the logarithmic function and the half-logistic form of the CDF of any continuous baseline distribution, raised to the power of pie. The newly introduced family is named the New Logarithmic Pie Power-G (NLPP-G) family of probability distributions. The main importance of the newly established method is that it does not require any extra parameters. The major outline of the presented study is as follows: Section 2 is based on the development of a new method and some key characteristics of the distribution family. Section 3 offers a special, versatile sub-model of the NLPP-G family of distributions called the New Logarithmic Pie Power Inverse Weibull (NLPP-IWD) distribution. Section 4 explores some fundamental properties of the NLPP-IWD in detail. In Sections 5 and 6, we discuss studies on model parameter estimation and simulation. Finally, A case study (two data sets are used to illustrate the practical performance) and concluding remarks are included in Sections 7 and 8.

2. The New Logarithmic Pie Power-G Family of Distributions

Using the logarithmic function and the half-logistic form of the CDF of the baseline distribution raised to the power of π, the present section proposes a novel approach to probability distributions known as the NLPP-G family. Let suppose $S(t;\tau)$ be the survival function (SF) of any candidate distributions having the PDF, $a(t;\tau)$; that is $S(t;\tau)=1-A(t;\tau)$. Then the CDF, $F(t;\tau)$, and the PDF, $f(t;\tau)$, of the NLPP-G method can be expressed as

$$F(t;\tau)=1-\frac{\log\left(\pi+\left(1-\pi^{\left(\frac{2A(t;\tau)}{1+A(t;\tau)}\right)}\right)\right)}{\log(\pi)}; \qquad t\in\Re, \tag{2.1}$$

$$f(t;\tau)=\frac{2a(t;\tau)\pi^{\left(\frac{2A(t;\tau)}{1+A(t;\tau)}\right)}}{\left(1+A(t;\tau)\right)^2\left(\pi+\left(1-\pi^{\left(\frac{2A(t;\tau)}{1+A(t;\tau)}\right)}\right)\right)}; \qquad t\in\Re, \tag{2.2}$$

where, $A(t;\tau)$ and $a(t;\tau)$ are the CDF and PDF of any base member depending on a vector of parameters $\tau\in\Re^+$. Further, to confirm the validity of the CDF $F(t;\tau)$ of the proposed family of distributions, we have two propositions that can be used for this purpose:

Proposition 1. For CDF $F(t;\tau)$ in Eq. (2.1), we need to prove the following two conditions

$$\lim_{t\to-\infty}F(t;\tau)=0, \text{ and } \lim_{t\to\infty}F(t;\tau)=1.$$

Proof. Link to Eq. (2.1), applying the limit, we have

$$\lim_{t\to-\infty}F(t;\tau)=1-\frac{\log\left(\pi+\left(1-\pi^{\left(\frac{2A(-\infty;\tau)}{1+A(-\infty;\tau)}\right)}\right)\right)}{\log(\pi)}, \tag{2.3}$$

if $A(t;\tau)$ is a real CDF of any base member, then

$$A(-\infty;\tau)=0\text{, and}$$

$$\lim_{t\to-\infty} F(t;\tau)=1-\frac{\log\left(\pi+\left(1-\pi^{0}\right)\right)}{\log(\pi)}, \tag{2.4}$$

$$\lim_{t\to-\infty} F(t;\tau)=0.$$

Again, applying the limit of Eq. (2.1), we have

$$\lim_{t\to\infty} F(t;\tau)=1-\frac{\log\left(\pi+\left(1-\pi^{\left(\frac{2A(\infty;\tau)}{1+A(\infty;\tau)}\right)}\right)\right)}{\log(\pi)}. \tag{2.5}$$

As, $A(t;\tau)$ is the CDF of baseline members, then

$$A(t;\tau)=1\text{, and}$$

$$\lim_{t\to\infty} F(t;\tau)=1-\frac{\log\left(\pi+\left(1-\pi\right)\right)}{\log(\pi)}, \tag{2.6}$$

after further simplification, we get

$$\lim_{t\to\infty} F(t;\tau)=1.$$

Proposition 2. The $A(t;\tau)$ is the CDF of any base distribution, right-continuous (non-negative), and differentiable.

Proof. $\frac{d}{dt}A(t;\tau)=a(t;\tau)$.

Hence, from the above discussion (i.e., propositions 1 and 2), it is observed that CDF $F(t;\tau)$ in Eq. (2.1) of the NLPP-G family of distributions is a valid CDF and very attractive. Similarly, corresponding to Eq. (2.1) and Eq. (2.2), the SF is represented as $S(t;\tau)=1-F(t;\tau)$, HF (hazard rate function) represented as $h(t;\tau)=\frac{f(t;\tau)}{S(t;\tau)}$, and CHF (cumulative HF) represented as $H(t;\tau)=-\log\left(S(t;\tau)\right)$ of the NLPP-G distributions family, respectively, are expressed in general by the following forms

$$S(t;\tau)=\frac{\log\left(\pi+\left(1-\pi^{\left(\frac{2A(t;\tau)}{1+A(t;\tau)}\right)}\right)\right)}{\log(\pi)}, \qquad t\in\Re, \tag{2.7}$$

$$h(t;\tau)=\frac{2\log(\pi)\,a(t;\tau)\,\pi^{\left(\frac{2A(t;\tau)}{1+A(t;\tau)}\right)}}{\left(1+A(t;\tau)\right)^{2}\log\left(\pi+\left(1-\pi^{\left(\frac{2A(t;\tau)}{1+A(t;\tau)}\right)}\right)\right)\left(\pi+\left(1-\pi^{\left(\frac{2A(t;\tau)}{1+A(t;\tau)}\right)}\right)\right)}, \qquad t\in\Re, \tag{2.8}$$

and

$$H(t;\tau)=-\log\left(\frac{\log\left(\pi+\left(1-\pi^{\left(\frac{2A(t;\tau)}{1+A(t;\tau)}\right)}\right)\right)}{\log(\pi)}\right),\qquad t\in\Re. \tag{2.9}$$

The QF (Quantile function) and RD (Random deviation) for the NLPP-G family of distributions can be derived as follows

$$Q_t(u)=A^{-1}\left[\frac{\log\left(1+\pi-e^{(1-u)\log(\pi)}\right)}{2\log(\pi)-\log\left(1+\pi-e^{(1-u)\log(\pi)}\right)}\right], \tag{2.10}$$

where $u\in(0,1)$, and

$$p=A^{-1}\left[\frac{\log\left(1+\pi-e^{(1-p)\log(\pi)}\right)}{2\log(\pi)-\log\left(1+\pi-e^{(1-p)\log(\pi)}\right)}\right]. \tag{2.11}$$

Similarly, using some algebraic expansions

$$(1-t)^n=\sum_{s=0}^{\infty}(-1)^s\binom{n}{s}t^s, \tag{2.12}$$

$$(1+t)^n=\sum_{c=0}^{\infty}(-1)^c\,t^c, \tag{2.13}$$

$$\pi^t=\sum_{h=0}^{\infty}\frac{(t\log\pi)^h}{h!}. \tag{2.14}$$

The PDF in relation to Eq. (2.2) can be derived in linear form as

$$f(t;\tau)=\sum_{s=0}^{\infty}\sum_{c=0}^{\infty}\sum_{h=0}^{\infty}\sum_{p=0}^{\infty}2^{h+1}\pi^{-s}(-1)^{s+c+h}(\log\pi)^h(1+c)^h\binom{s}{c}\binom{h+p+1}{p}A^{h+l}(t;\tau)a(t;\tau),$$

$$f(t;\tau)=\sum_{s=0}^{\infty}\sum_{c=0}^{\infty}\sum_{h=0}^{\infty}\sum_{p=0}^{\infty}\Psi_{s,c,h,p}A^{h+l}(t;\tau)a(t;\tau), \tag{2.15}$$

where, $\Psi_{s,c,h,p}=2^{h+1}\pi^{-i}(-1)^{s+c+h}(\log\pi)^c(1+h)^c\binom{s}{h}\binom{c+p+1}{p}$.

In the next section, we implement the proposed method and suggest a novel logarithmic and transformation form of the traditional Inverse Weibull probability model, known as the New Logarithmic Pie Power Inverse Weibull (NLPP-IW) probability model. In the same Section, some visual representations of the CDF, PDF, SF, and HF are also visualized.

3. NLPP-IW Distribution

Suppose that $t\left(\in\Re^+\right)$ be a RV (random variable) that follows an Inverse Weibull model with parameters $\beta>0$ and $\phi>0$. Then it's CDF, $A(t;\tau)$, is expressed by

$$A(t;\tau)=e^{-\delta t^{-\phi}},\qquad t\geq 0, \tag{3.1}$$

with the PDF, $a(t;\tau)$, corresponding to Eq. (3.1), is presented by

$$a(t;\tau)=\phi\delta t^{-(\phi+1)}e^{-\delta t^{-\phi}}, \qquad t>0. \qquad (3.2)$$

Substituting Eq. (3.1) in Eq. (2.1), we acquire the CDF, $F(t;\tau)$, of our proposed NLPP-IWD as follows

$$F(t;\tau)=1-\frac{\log\left(\pi+\left(1-\pi^{\left(\frac{2e^{-\delta t^{-\phi}}}{1+e^{-\delta t^{-\phi}}}\right)}\right)\right)}{\log(\pi)}, \qquad t\geq 0, \qquad (3.3)$$

the PDF $f(t;\tau)$ related to Eq. (8) of the NLPP-IWD can be stated as

$$f(t;\tau)=\frac{2\phi\delta t^{-(\phi+1)}\left(1+e^{-\delta t^{-\phi}}\right)^{-2}e^{-\delta t^{-\phi}}\pi^{\left(\frac{2e^{-\delta t^{-\phi}}}{1+e^{-\delta t^{-\phi}}}\right)}}{\left(\pi+\left(1-\pi^{\left(\frac{2e^{-\delta t^{-\phi}}}{1+e^{-\delta t^{-\phi}}}\right)}\right)\right)}, \qquad t>0. \qquad (3.4)$$

Similarly, the SF $S(t;\tau)$, HF $h(t;\tau)$, and $H(t;\tau)$ CHF of the NLPP-IWD is as follows

$$S(t;\tau)=\frac{\log\left(\pi+\left(1-\pi^{\left(\frac{2e^{-\delta t^{-\phi}}}{1+e^{-\delta t^{-\phi}}}\right)}\right)\right)}{\log(\pi)}, \qquad t>0, \qquad (3.5)$$

$$h(t;\tau)=\frac{2\delta\phi t^{-(\phi+1)}\left(e^{-\delta t^{-\phi}}+1\right)^{-2}e^{-\delta t^{-\phi}}\pi^{\left(\frac{2e^{-\delta t^{-\phi}}}{1+e^{-\delta t^{-\phi}}}\right)}}{\left(\pi+\left(1-\pi^{\left(\frac{2e^{-\delta t^{-\phi}}}{1+e^{-\delta t^{-\phi}}}\right)}\right)\right)\log\left(\pi+\left(1-\pi^{\left(\frac{2e^{-\delta t^{-\phi}}}{1+e^{-\delta t^{-\phi}}}\right)}\right)\right)}, \qquad t>0, \qquad (3.6)$$

and

$$H(t;\tau)=\log\left(\frac{\log\left(\pi+\left(1-\pi^{\left(\frac{2e^{-\delta t^{-\phi}}}{1+e^{-\delta t^{-\phi}}}\right)}\right)\right)}{\log(\pi)}\right), \qquad t>0. \qquad (3.7)$$

The CDF, $F(t;\tau)$, and SF, $S(t;\tau)$, plots of the NLPP-IW distribution are graphically illustrated in Figure 1. From Figure 1, we can see that the SF, $S(t;\tau)$, the (right panel) plots is the opposite of the CDF, $F(t;\tau)$, the (left panel) plots, then, from Figure 1, it is also determined that the CDF, $F(t;\tau)$, of the newly derived distribution is a real (or valid) CDF.

Similarly, the PDF, $f(t;\tau)$, and HF, $h(t;\tau)$, plots of the NLPP-IWD are also graphically illustrated in Figure 2. The PDF, $f(t;\tau)$, plots of the NLPP-IWD can take different positively skewed patterns, and Figure 2 (left panel) shows these diverse patterns. On the other hand, the HF, $h(t;\tau)$, plots of the NLPP-IWD can also take different kinds of non-monotonic shapes, such as decreasing, increasing, reversed J shapes, and upside-down bathtub shapes. Figure 2 (right panel) shows these diverse patterns. Hence, from these plots, it is observed that the NLPP-IWD is more versatile and can be a suitable contender for modeling right (or positively) skewed datasets.

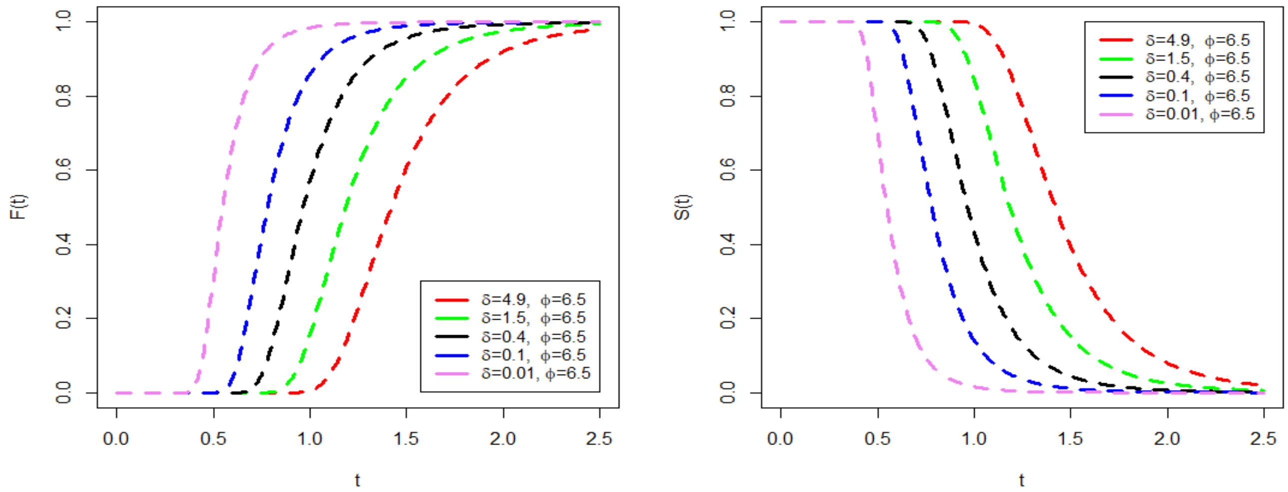

Figure 1: Various shapes of $F(t;\tau)$ and $S(t;\tau)$, of the NLPP-IWD.

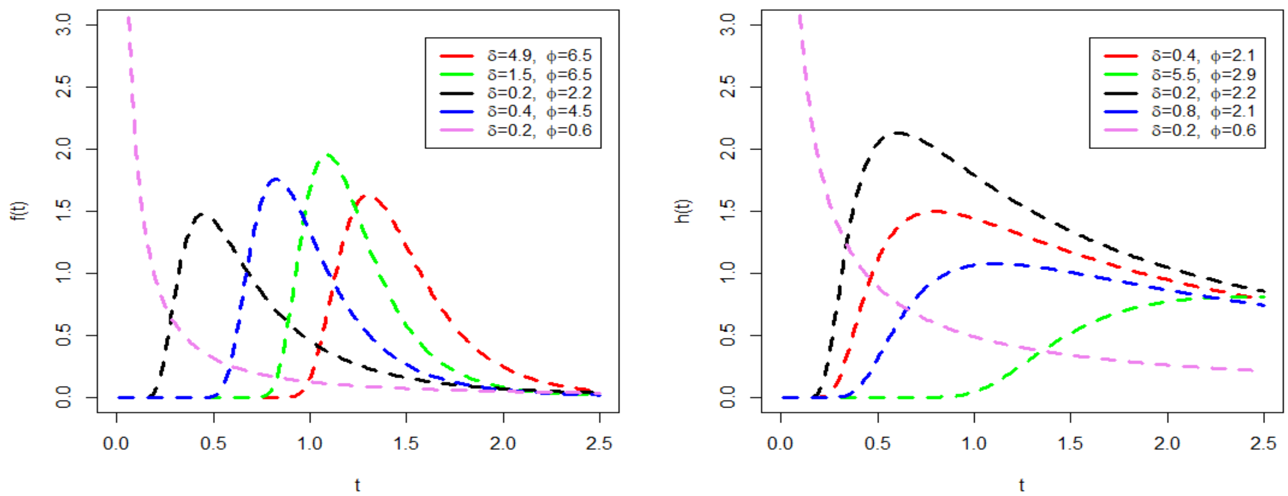

Figure 2: Various shapes of the PDF, $f(t;\tau)$, and HF, $h(t;\tau)$, of the NLPP-IWD.

Furthermore, the Quantile function, say $Q_t(u)$, of the NLPP-IWD can be stated in the following form

$$Q_t(u)=\left[\frac{-1}{\delta}\log\left\{\frac{\log\left(1+\pi-e^{(1-u)\log(\pi)}\right)}{2\log(\pi)-\log\left(1+\pi-e^{(1-u)\log(\pi)}\right)}\right\}\right]^{-1/\phi}, \qquad u\in(0,1). \tag{3.8}$$

Similarly, Bowley's skewness and Moors kurtosis based on the quantile function are stated as follows

$$SK_B=\frac{Q(0.75)-2Q(0.5)+Q(0.25)}{Q(0.75)-Q(0.25)}, \tag{3.9}$$

$$KU_M=\frac{Q(0.875)-Q(0.625)-Q(0.125)+Q(0.375)}{Q(0.75)-Q(0.25)}. \tag{3.10}$$

Likewise, linked to Eq. (3.4) and after mathematical calculation of the PDF, $f(t;\tau)$, of the NLPP-IWD may be obtained in a linear form as

$$f(t;\tau)=\sum_{s=0}^{\infty}\sum_{c=0}^{\infty}\sum_{h=0}^{\infty}\sum_{p=0}^{\infty}\Psi_{s,c,h,p}\,\phi\delta t^{-(\phi+1)}e^{-(h+p+1)\delta t^{-\phi}}, \tag{3.11}$$

$$f(t;\tau)=\sum_{s=0}^{\infty}\sum_{c=0}^{\infty}\sum_{h=0}^{\infty}\sum_{p=0}^{\infty}\Psi^{*}_{s,c,h,p}\,t^{-(\phi+1)}e^{-(h+p+1)\delta t^{-\phi}}, \tag{3.12}$$

where, $\Psi^{*}_{s,c,h,p}=\aleph_{s,c,h,p}\delta\phi$, and $\Psi_{s,c,h,p}=2^{h+1}\pi^{-s}(-1)^{s+c+h}(\log\pi)^{h}(1+c)^{h}\binom{s}{c}\binom{h+p+1}{p}$.

4. Statistical Properties

Next, the present section of the article is based on the establishment of statistical properties (or characteristics) of the NLPP-IWD, including Moments, MGF (moment generating functions), Incomplete-Moments, CF (characteristic function), MRL (mean residual life), and OS (Order Statistics).

4.1. Moments

Using moments, we may compute several statistical measures to characterize a distribution's shape and properties, including variance, skewness, kurtosis, and center tendency (or mean). Additionally, moments are also helpful for risk management, probability distribution comparison, and data summary. Let T be a RV and follow the NLPP-IWD with parameters δ, and ϕ linked to Eq. (3.12), then the corresponding rth moments, say $E(T^r)$, can be calculated as

$$E(T^r)=\sum_{s=0}^{\infty}\sum_{c=0}^{\infty}\sum_{h=0}^{\infty}\sum_{p=0}^{\infty}\Psi^{*}_{s,c,h,p}\int_0^{\infty}t^{r-\phi-1}e^{-(h+p+1)\delta t^{-\phi}}dt, \tag{4.1}$$

$$E(T^r)=\sum_{s=0}^{\infty}\sum_{c=0}^{\infty}\sum_{h=0}^{\infty}\sum_{p=0}^{\infty}\Psi^{*}_{s,c,h,p}\int_0^{\infty}w^{-\frac{r}{\phi}+1-1}e^{-(h+p+1)\delta w}dw, \tag{4.2}$$

$$E(T^r)=\sum_{s=0}^{\infty}\sum_{c=0}^{\infty}\sum_{h=0}^{\infty}\sum_{p=0}^{\infty}\Psi^{*}_{s,c,h,p}\frac{\phi^{-1}\Gamma\left(-\frac{r}{\phi}+1\right)}{\left((p+h+1)\delta\right)^{-\frac{r}{\phi}+1}}, \tag{4.3}$$

$$E\left(T^r\right)=\sum_{s=0}^{\infty}\sum_{c=0}^{\infty}\sum_{h=0}^{\infty}\sum_{p=0}^{\infty}\Psi^*_{s,c,h,p}\frac{\phi^{-1}\Gamma\left(\frac{\phi-r}{\phi}\right)}{\left(\left(p+h+1\right)\delta\right)^{\frac{\phi-r}{\phi}}};\qquad \phi>r. \tag{4.4}$$

Applying Eq. (4.4), the corresponding mean and variance of the NLPP-IWD can be calculated in the following forms. Furthermore, the numerical descriptions of the mean, second raw moment, skewness, variance, and kurtosis with diverse presumed values of their respective parameters of the NLPP-IWD are recorded in Table 1. From Table 1, we can see that the NLPP-IWD exhibits positive skewness (i.e., skewness > 0) and a leptokurtic (i.e., kurtosis > 3) distribution. Hence, the NLPP-IWD distribution is more versatile and can be used as a good contender for modelling skewed right-tailed datasets.

$$E\left(T\right)=\sum_{s=0}^{\infty}\sum_{c=0}^{\infty}\sum_{h=0}^{\infty}\sum_{p=0}^{\infty}\Psi^*_{s,c,h,p}\frac{\phi^{-1}\Gamma\left(\frac{\phi-1}{\phi}\right)}{\left(\left(h+p+1\right)\delta\right)^{\frac{\phi-1}{\phi}}};\qquad \phi>1, \tag{4.5}$$

and

$$E\left(T^2\right)=\sum_{s=0}^{\infty}\sum_{c=0}^{\infty}\sum_{h=0}^{\infty}\sum_{p=0}^{\infty}\Psi^*_{s,c,h,p}\frac{\phi^{-1}\Gamma\left(\frac{\phi-2}{\phi}\right)}{\left(\left(h+p+1\right)\delta\right)^{\frac{\phi-2}{\phi}}};\qquad \phi>2. \tag{4.6}$$

$$V\left(T\right)=E\left(T^2\right)-E\left(T\right)^2,$$

$$V\left(T\right)=\sum_{s=0}^{\infty}\sum_{c=0}^{\infty}\sum_{h=0}^{\infty}\sum_{p=0}^{\infty}\Psi^*_{s,c,h,p}\frac{\phi^{-1}\Gamma\left(\frac{\phi-2}{\phi}\right)}{\left(\left(h+p+1\right)\delta\right)^{\frac{\phi-2}{\phi}}}-\left[\sum_{s=0}^{\infty}\sum_{c=0}^{\infty}\sum_{h=0}^{\infty}\sum_{p=0}^{\infty}\Psi^*_{s,c,h,p}\frac{\phi^{-1}\Gamma\left(\frac{\phi-1}{\phi}\right)}{\left(\left(h+p+1\right)\delta\right)^{\frac{\phi-1}{\phi}}}\right]^2;\ \phi>2. \tag{4.7}$$

Table 1: Some descriptive metrics using various parameter value combinations.

δ	ϕ	E(X)	E(X²)	V(X)	Skewness	Kurtosis
1.000	5.500	1.215543	1.605561	0.1280171	2.918103	29.14362
1.000	5.900	1.210527	1.586848	0.1214721	2.852649	27.40497
1.000	6.500	1.17399	1.458196	0.0799433	2.423073	18.36239
1.200	5.500	1.256513	1.715616	0.1367921	2.918103	29.14362
1.200	5.900	1.234334	1.63485	0.1112690	2.681870	23.36001
1.200	6.500	1.207386	1.542337	0.0845562	2.423073	18.36238
2.260	6.550	1.327107	1.861189	0.0999761	2.401699	18.00099
2.890	7.220	1.335236	1.863872	0.0810156	2.204284	14.97781
2.990	7.880	1.306884	1.771525	0.0635802	2.057127	13.05325
4.330	8.440	1.340056	1.853031	0.0572817	1.958578	11.90107
4.550	8.560	1.342045	1.856751	0.0556671	1.939877	11.69387
4.770	8.990	1.329399	1.816281	0.0489789	1.878632	11.03951
4.880	9.660	1.305403	1.744376	0.0402979	1.798018	10.23234

0.110	9.780	0.882793	0.797259	0.0179365	1.785158	10.10902
0.550	11.550	1.032929	1.084046	0.0171038	1.635147	8.770292
0.770	14.770	1.047947	1.108609	0.0104163	1.472846	7.527700
0.760	25.880	1.025439	1.054625	0.0030993	1.253893	6.129850
0.660	26.990	1.013951	1.029637	0.0015413	1.179927	5.726343
0.980	28.550	1.032058	1.067708	0.0025654	1.228846	5.990840

4.2. Moments generating function

The MGF can also be used to calculate different moments. Furthermore, it is also essential to establish the distribution of the sum of IRV (independent RV), demonstrate the central limit theorem, and analyze the convergence characteristics of random variable sequences. Using Eq. (3.12), the MGF of the NLPP-IWD, say $M_t(y)$, can be defined as

$$M_t(y)=\sum_{s=0}^{\infty}\sum_{c=0}^{\infty}\sum_{h=0}^{\infty}\sum_{p=0}^{\infty}\sum_{q=0}^{\infty}\Psi^*{}_{s,c,h,p}\frac{y^q}{q!}\int_0^{\infty}t^{r-\phi-1}e^{-(h+p+1)\delta t^{-\phi}}dt, \tag{4.8}$$

$$M_t(y)=\sum_{s=0}^{\infty}\sum_{c=0}^{\infty}\sum_{h=0}^{\infty}\sum_{p=0}^{\infty}\sum_{q=0}^{\infty}\Psi^*{}_{s,c,h,p}\frac{y^q}{q!}\int_0^{\infty}w^{-\frac{r}{\phi}+1-1}e^{-(h+p+1)\delta w}dw, \tag{4.9}$$

$$M_t(y)=\sum_{s=0}^{\infty}\sum_{c=0}^{\infty}\sum_{h=0}^{\infty}\sum_{p=0}^{\infty}\sum_{q=0}^{\infty}\Psi^*{}_{s,c,h,l}\frac{y^q}{q!}\frac{\phi^{-1}\Gamma\left(-\frac{r}{\phi}+1\right)}{\left((h+p+1)\delta\right)^{-\frac{r}{\phi}+1}}, \tag{4.10}$$

$$M_t(y)=\sum_{s=0}^{\infty}\sum_{c=0}^{\infty}\sum_{h=0}^{\infty}\sum_{p=0}^{\infty}\sum_{q=0}^{\infty}\Psi^*{}_{s,c,h,l}\frac{y^q}{q!}\frac{\phi^{-1}\Gamma\left(\frac{\phi-r}{\phi}\right)}{\left((h+p+1)\delta\right)^{\frac{\phi-r}{\phi}}};\qquad \phi>r. \tag{4.11}$$

4.3. Incomplete moments

Applying Eq. (3.12), the IM (incomplete moments) of the NLPP-IWD say $M_r(x)$, can be stated as

$$M_r(x)=\sum_{s=0}^{\infty}\sum_{c=0}^{\infty}\sum_{h=0}^{\infty}\sum_{p=0}^{\infty}\Psi^*{}_{s,c,h,p}\int_0^{x}t^{r-\phi-1}e^{-(h+p+1)\delta t^{-\phi}}dt, \tag{4.12}$$

$$M_r(x)=\sum_{s=0}^{\infty}\sum_{c=0}^{\infty}\sum_{h=0}^{\infty}\sum_{p=0}^{\infty}\Psi^*{}_{s,c,h,p}\frac{\phi^{-1}\left[\gamma\left(\frac{\phi-r}{\phi},(h+p+1)\delta x^{-\phi}\right)\right]}{\left((h+p+1)\delta\right)^{\frac{\phi-r}{\phi}}};\qquad \phi>r, \tag{4.13}$$

where, $\gamma(.)$ is the incomplete GF (gamma function).

4.4. Characteristics function

The CF can be used to investigate the limit theorems and examine the characteristics of probability distributions. It is also applicable in many more fields, such as signal processing and quantum mechanics. So, using Eq. (3.12), the CF of the NLPP-IWD say $\Phi_t(y)$, can be specified as

$$\Phi_t(y)=\sum_{s=0}^{\infty}\sum_{c=0}^{\infty}\sum_{h=0}^{\infty}\sum_{p=0}^{\infty}\sum_{q=0}^{\infty}\Psi^*{}_{s,c,h,p}\frac{(vy)^q}{q!}\int_0^{\infty}t^{r-\phi-1}e^{-(h+p+1)\delta t^{-\phi}}dt, \tag{4.14}$$

$$\Phi_t(y)=\sum_{s=0}^{\infty}\sum_{c=0}^{\infty}\sum_{h=0}^{\infty}\sum_{p=0}^{\infty}\sum_{q=0}^{\infty}\Psi^*_{s,c,h,p}\frac{(vy)^q}{q!}\frac{\phi^{-1}\Gamma\left(\frac{\phi-r}{\phi}\right)}{\left((h+p+1)\delta\right)^{\frac{\phi-r}{\phi}}}\ ;\ \phi>r\ , \tag{4.15}$$

where, $v=\sqrt{-1}$.

4.5. Mean residual life

In actuarial, engineering, and medical sciences, the MRL is used to model lifetime and predict or forecast future performance based on current age or survival time. Using Eq. (3.12), the corresponding MRL of the NLPP-IWD say $\overline{M(x)}$, can be derived as

$$\overline{M(x)}=\frac{1}{G(x)}\left[\mu-\sum_{s=0}^{\infty}\sum_{c=0}^{\infty}\sum_{h=0}^{\infty}\sum_{p=0}^{\infty}\Psi^*_{s,c,h,p}\int_0^x t^{r-\phi-1}e^{-(h+p+1)\delta t^{-\phi}}dt\right]-x\ , \tag{4.16}$$

$$\overline{M(x)}=\frac{1}{G(x)}\left[\mu-\sum_{s=0}^{\infty}\sum_{c=0}^{\infty}\sum_{h=0}^{\infty}\sum_{p=0}^{\infty}\Psi^*_{s,c,h,p}\frac{\phi^{-1}\left[\gamma\left(\frac{\phi-r}{\phi},(h+p+1)\delta x^{-\phi}\right)\right]}{\left((h+p+1)\delta\right)^{\frac{\phi-r}{\phi}}}\right]-x\ , \tag{4.17}$$

where, $\gamma(.)$ is the incomplete gamma function.

4.6. Order statistics

Let $T_1,T_2,...,T_n$ be the random samples (RS) of size n drawn from the NLPP-IWD with PDF $f(t;\tau)$ and CDF $F(t;\tau)$, then the related density function of the wth OS is presented by

$$f_{w:n}(t)=\frac{n!}{(w-1)!(n-w)!}F(t;\tau)^{w-1}f(t;\tau)\left(1-F(t;\tau)\right)^{n-w}. \tag{4.18}$$

Inserting Eq. (3.3) and Eq. (3.4) in Eq. (4.18), the we get

$$f_{w:n}(t)=\frac{n!}{(w-1)!(n-w)!}\frac{2\delta\phi t^{-(\phi+1)}\left(1+e^{-\delta t^{-\phi}}\right)^{-2}e^{-\delta t^{-\phi}}\pi^{\left(\frac{2e^{-\delta t^{-\phi}}}{1+e^{-\delta t^{-\phi}}}\right)}}{\left(\pi+\left(1-\pi^{\left(\frac{2e^{-\delta t^{-\phi}}}{1+e^{-\delta t^{-\phi}}}\right)}\right)\right)}$$

$$\times\left[1-\frac{\log\left(\pi+\left(1-\pi^{\left(\frac{2e^{-\delta t^{-\phi}}}{1+e^{-\delta t^{-\phi}}}\right)}\right)\right)}{\log(\pi)}\right]^{w-1}\left[\frac{\log\left(\pi+\left(1-\pi^{\left(\frac{2e^{-\delta t^{-\phi}}}{1+e^{-\delta t^{-\phi}}}\right)}\right)\right)}{\log(\pi)}\right]^{n-w} \tag{4.19}$$

The CDF $F_{1:n}(t)$ and PDF $f_{1:n}(t)$ of the first-OS are given by

$$F_{1:n}(t)=\left[\frac{\log\left(\pi+\left(1-\pi^{\left(\frac{2e^{-\delta t^{-\phi}}}{1+e^{-\delta t^{-\phi}}}\right)}\right)\right)}{\log(\pi)}\right]^{n}; \qquad t>0. \tag{4.20}$$

And

$$f_{1:n}(t)=\frac{2n\delta\phi t^{-(\phi+1)}\left(1+e^{-\delta t^{-\phi}}\right)^{-2}e^{-\delta t^{-\phi}}\pi^{\left(\frac{2e^{-\delta t^{-\phi}}}{e^{-\delta t^{-\phi}}+1}\right)}}{\left(\pi+\left(1-\pi^{\left(\frac{2e^{-\delta t^{-\phi}}}{e^{-\delta t^{-\phi}}+1}\right)}\right)\right)}\left[\frac{\log\left(\pi+\left(1-\pi^{\left(\frac{2e^{-\delta t^{-\phi}}}{1+e^{-\delta t^{-\phi}}}\right)}\right)\right)}{\log(\pi)}\right]^{n-1}; \qquad t>0. \tag{4.21}$$

The CDF $F_{n:n}(t)$ and PDF $f_{n:n}(t)$ of OS at the n[th] level are provided by

$$F_{n:n}(t)=\left[1-\frac{\log\left(\pi+\left(1-\pi^{\left(\frac{2e^{-\delta t^{-\phi}}}{1+e^{-\delta t^{-\phi}}}\right)}\right)\right)}{\log(\pi)}\right]^{n}; \qquad t>0. \tag{4.22}$$

And

$$f_{n:n}(t)=\frac{2n\delta\phi t^{-(\phi+1)}\left(1+e^{-\delta t^{-\phi}}\right)^{-2}e^{-\delta t^{-\phi}}\pi^{\left(\frac{2e^{-\delta t^{-\phi}}}{e^{-\delta t^{-\phi}}+1}\right)}}{\left(\pi+\left(1-\pi^{\left(\frac{2e^{-\delta t^{-\phi}}}{1+e^{-\delta t^{-\phi}}}\right)}\right)\right)}\left[1-\frac{\log\left(\pi+\left(1-\pi^{\left(\frac{2e^{-\delta t^{-\phi}}}{1+e^{-\delta t^{-\phi}}}\right)}\right)\right)}{\log(\pi)}\right]^{n-1}; \qquad t>0. \tag{4.23}$$

5. Estimation

In the present section, the corresponding model parameters of the NLPP-IWD are estimated through the MLE (maximum likelihood estimation) scheme. Let $T_1, T_2, ..., T_n$ be the set of RS of size n randomly selected or taken from NLPP-IWD, with observed values assumed by $t_1, t_2, ..., t_n$, then the corresponding LLF (Log-likelihood-function) associated with Eq. (3.4), is given by

$$\ell(t)=n\log(2\delta\phi)-(\phi+1)\sum_{i=1}^{n}\log t_i-2\sum_{i=1}^{n}\log\left(1+e^{-\delta t_i^{-\phi}}\right)$$
$$-\delta\sum_{i=1}^{n}t_i^{-\phi}+\log(\pi)\sum_{i=1}^{n}\left(\frac{2e^{-\delta t_i^{-\phi}}}{1+e^{-\delta t_i^{-\phi}}}\right)-\sum_{i=1}^{n}\log\left(\pi+\left(1-\pi^{\left(\frac{2e^{-\delta t_i^{-\phi}}}{1+e^{-\delta t_i^{-\phi}}}\right)}\right)\right). \quad (5.1)$$

The partial derivative of Eq. (5.1) concerning δ and ϕ are given by

$$\frac{d\ell(t)}{d\delta}=\frac{n}{\delta}+2\sum_{i=1}^{n}\frac{t_i^{-\phi}e^{-\delta t_i^{-\phi}}}{\left(1+e^{-\delta t_i^{-\phi}}\right)}-\sum_{i=1}^{n}t_i^{-\phi}-\log(\pi)2\sum_{i=1}^{n}\frac{t_i^{-\phi}e^{-\delta t_i^{-\phi}}}{\left(1+e^{-\delta t_i^{-\phi}}\right)^2}+\sum_{i=1}^{n}\frac{\log(\pi)t_i^{-\phi}e^{-\delta t_i^{-\phi}}\pi^{\left(\frac{2e^{-\delta t_i^{-\phi}}}{1+e^{-\delta t_i^{-\phi}}}\right)}}{\left(\pi+\left(1-\pi^{\left(\frac{2e^{-\delta t_i^{-\phi}}}{1+e^{-\delta t_i^{-\phi}}}\right)}\right)\right)\left(1+e^{-\delta t_i^{-\phi}}\right)^2}, (5.2)$$

$$\frac{d\ell(t)}{d\phi}=\frac{n}{\phi}-\sum_{i=1}^{n}\log t_i+2\sum_{i=1}^{n}\frac{\log(t_i)\delta t_i^{-\phi}e^{-\delta t_i^{-\phi}}}{\left(1+e^{-\delta t_i^{-\phi}}\right)}+\delta\sum_{i=1}^{n}\log(t_i)t_i^{-\phi}+2\log(\pi)\sum_{i=1}^{n}\frac{\delta\log(t_i)t_i^{-\phi}e^{-\delta t_i^{-\phi}}}{\left(1+e^{-\delta t_i^{-\phi}}\right)^2}$$
$$+2\sum_{i=1}^{n}\frac{\log(\pi)\delta\log(t_i)t_i^{-\phi}e^{-\delta t_i^{-\phi}}\pi^{\left(\frac{2e^{-\delta t_i^{-\phi}}}{1+e^{-\delta t_i^{-\phi}}}\right)}}{\left(\pi+\left(1-\pi^{\left(\frac{2e^{-\delta t_i^{-\phi}}}{1+e^{-\delta t_i^{-\phi}}}\right)}\right)\right)\left(e^{-\delta t_i^{-\phi}}+1\right)^2}. \quad (5.3)$$

By using appropriate software and setting $\frac{\partial\ell(t)}{\partial\delta}=0$, and $\frac{\partial\ell(t)}{\partial\phi}=0$, one can easily obtain the estimates based on the MLE method.

6. Simulations

This section of the paper is based on the MCSS (Monte Carlo Simulation-Study) to judge the effectiveness of the MLEs $\left(\hat{\delta}_{MLE},\hat{\phi}_{MLE}\right)$ method for the NLPP-IWD. For simulation analysis, use Eq. (3.8) to generate a random sample from the NLPP-IWD. Four sets of different combinations of parameter values of the NLPP-IWD, such as Set I (δ,ϕ): (2.80, 2.70), Set II (δ,ϕ): (1.75, 2.75), Set III (δ,ϕ): (2.33, 3.44), Set IV (δ,ϕ): (2.93, 2.64), Set V (δ,ϕ): (3.50, 3.20), and Set VI (δ,ϕ): (3.10, 1.70) are employed. For the simulation study, it is important to note that there are no strict or mild limitations on selecting the model parameter values. Random samples of sizes, say, 25, 75, 100, 200, 400, 600, 700, 800, 900, and 1000, are generated from NLPP-IWD, and the whole process for each sample is repeated 1000 times. We considered the estimates of MLEs, biases, and MSE as the pivotal tools to examine the performance of MLEs $\left(\hat{\delta}_{MLE},\hat{\phi}_{MLE}\right)$ of the NLPP-IWD. The simulation process is carried out by using the well-known R language software (Core Team, 2023, version 4.2.3) with the rootSolve package. The decisive tools with mathematical expression, respectively, given by

$$Bias(\Delta)=\frac{1}{800}\sum_{i=1}^{800}(\hat{\Delta}-\Delta)$$

and

$$MSE(\Delta) = \frac{1}{800}\sum_{i=1}^{800}(\hat{\Delta}-\Delta)^2 ,$$

where, $\Delta = (\delta, \phi)$.

Table 2: The MLEs, Biases, and MSEs results for Sets I and II.

		Set I: $\delta = 2.80, \phi = 2.70$			Set II: $\delta = 1.75, \phi = 2.75$		
n	Est.	MLEs	MSEs	Biases	MLEs	MSEs	Biases
25	$\hat{\delta}$	4.013130	0.97168328	0.35793020	1.926439	1.022326279	0.17643852
	$\hat{\phi}$	2.859115	0.21268510	0.15911527	2.913583	0.261149237	0.16358257
75	$\hat{\delta}$	2.881349	0.20674054	0.08134861	1.794561	0.068838373	0.04456133
	$\hat{\phi}$	2.745158	0.06300273	0.04515763	2.796166	0.063059311	0.04616570
100	$\hat{\delta}$	2.879022	0.15865863	0.07902211	1.780957	0.044157308	0.03095734
	$\hat{\phi}$	2.735343	0.04657398	0.03534305	2.788926	0.049272393	0.03892647
200	$\hat{\delta}$	2.847707	0.07688929	0.04770658	1.763732	0.020913451	0.01373212
	$\hat{\phi}$	2.720558	0.02053382	0.02055834	2.773738	0.022759887	0.02373762
300	$\hat{\delta}$	2.824695	0.04708719	0.02469485	1.766131	0.014232330	0.01613064
	$\hat{\phi}$	2.712142	0.01469977	0.01214169	2.762044	0.015777172	0.01204404
400	$\hat{\delta}$	2.818302	0.03609039	0.01830155	1.756656	0.010926919	0.00665620
	$\hat{\phi}$	2.709964	0.01064049	0.00996377	2.762193	0.011356452	0.01219301
500	$\hat{\delta}$	2.815989	0.02893085	0.01598928	1.758926	0.007969159	0.00892591
	$\hat{\phi}$	2.704044	0.00855818	0.00404416	2.758146	0.008658632	0.00814582
600	$\hat{\delta}$	2.812696	0.02098417	0.01269649	1.754136	0.007095645	0.00413551
	$\hat{\phi}$	2.709836	0.00654413	0.00983625	2.757545	0.007779853	0.00754489
700	$\hat{\delta}$	2.812427	0.01811085	0.01242655	1.752931	0.006011428	0.00393092
	$\hat{\phi}$	2.704259	0.00547070	0.00425923	2.752853	0.005969711	0.00685295
800	$\hat{\delta}$	2.807869	0.01560433	0.00995367	1.755671	0.005318917	0.00365549
	$\hat{\phi}$	2.699867	0.00517608	0.00394174	2.748985	0.005402041	0.00580662
900	$\hat{\delta}$	2.812495	0.01500809	0.00509530	1.751936	0.004663104	0.00182568
	$\hat{\phi}$	2.705156	0.00434464	0.00315560	2.755645	0.005147133	0.00605762
1000	$\hat{\delta}$	2.805922	0.01313622	0.00402224	1.755298	0.003725304	0.00129844
	$\hat{\phi}$	2.703020	0.00382739	0.00302015	2.751715	0.004563882	0.00271503

Table 3: The MLEs, Biases, and MSEs results for Sets III and IV.

n	Est.	Set III: $\delta = 2.33, \phi = 3.44$			Set IV: $\delta = 2.93, \phi = 2.64$		
		MLEs	MSEs	Biases	MLEs	MSEs	Biases
25	$\hat{\delta}$	2.603074	1.02456571	0.28632971	3.278873	1.07493919	0.36213551
	$\hat{\phi}$	3.627329	0.35020209	2.07411e-01	2.773500	0.20817826	0.14474667
75	$\hat{\delta}$	2.418520	0.14653108	0.08438549	3.022551	0.25885893	0.09089114
	$\hat{\phi}$	3.509389	0.08805449	5.63828e-02	2.693742	0.05931741	0.03520490
100	$\hat{\delta}$	2.373835	0.09505424	0.06746943	2.993822	0.17643814	0.08599645
	$\hat{\phi}$	3.473496	0.07699354	5.37270e-02	2.661881	0.04316312	0.04161532
200	$\hat{\delta}$	2.347616	0.04682980	0.01799097	2.951757	0.08137917	0.05171889
	$\hat{\phi}$	3.447337	0.03359952	1.70286e-02	2.645406	0.02178252	0.02295061
300	$\hat{\delta}$	2.342860	0.03231351	0.02540161	2.932699	0.05632679	0.02518787
	$\hat{\phi}$	3.442362	0.02394606	1.35044e-02	2.644743	0.01419824	0.01312479
400	$\hat{\delta}$	2.335687	0.01960094	0.01768583	2.929114	0.03872287	0.02454034
	$\hat{\phi}$	3.449792	0.01719335	1.18430e-02	2.645781	0.01004036	0.01246110
500	$\hat{\delta}$	2.338671	0.01579873	0.00867052	2.942037	0.02803798	0.01203650
	$\hat{\phi}$	3.446145	0.01309880	6.14527e-03	2.646899	0.00777855	0.00689863
600	$\hat{\delta}$	2.343690	0.01454011	0.01369028	2.942212	0.02463613	0.01156304
	$\hat{\phi}$	3.455486	0.01248037	1.54850e-02	2.642054	0.00642284	0.00994672
700	$\hat{\delta}$	2.334984	0.01180461	0.00498449	2.942137	0.02212512	0.01067374
	$\hat{\phi}$	3.445758	0.00951602	5.75851e-03	2.641538	0.00571398	0.00599749
800	$\hat{\delta}$	2.338533	0.01060911	0.00853254	2.941320	0.01854917	0.01032007
	$\hat{\phi}$	3.451955	0.00853477	1.19518e-02	2.642849	0.00475389	0.00284902
900	$\hat{\delta}$	2.337923	0.00883684	0.00792287	2.944978	0.01647234	0.00625113
	$\hat{\phi}$	3.441691	0.00745735	1.69163e-03	2.645297	0.00414293	0.00104365
1000	$\hat{\delta}$	2.335468	0.00851195	0.00546828	2.939104	0.01521736	0.00410438
	$\hat{\phi}$	3.447781	0.00711023	7.78146e-03	2.643508	0.00370252	0.00350787

Linked to set I(δ,ϕ), set II $(\phi;\delta)$, set III (δ,ϕ), set IV (δ,ϕ), set V (δ,ϕ), and set VI (δ,ϕ), the numerical results of the simulation analysis are presented in Tables 2, 3, and 4. From Tables 2-4, we can see that as the sample size increased (i.e., $n \to \infty$), the MLE values of $\hat{\delta}_{MLE}$, and $\hat{\phi}_{MLE}$ become constant and approach the true parameter values. Similarly, the MSE values of $\hat{\phi}_{MLE}$ and $\hat{\delta}_{MLE}$ decreases, and Biases of the $\hat{\delta}_{MLE}$, and $\hat{\phi}_{MLE}$ are also gradually approaching zero as the sample size increases. Numerically and graphically, it is observed that the employed MLE method demonstrates asymptotic efficiency, consistency and upholds the invariance property. Hence, the MLE method provides a suitable approach for estimating the model parameters corresponding to the proposed method.

Table 4: The MLEs, Biases, and MSEs results for Sets V and VI.

n	Est.	Set V: $\delta = 3.50, \phi = 3.20$			Set VI: $\delta = 3.10, \phi = 1.70$		
		MLEs	MSEs	Biases	MLEs	MSEs	Biases
25	$\hat{\delta}$	3.778969	1.03682626	0.27896921	3.423361	1.02822279	0.32336126
	$\hat{\phi}$	3.326114	0.24557899	0.12611422	1.774880	0.07849702	0.07488001
75	$\hat{\delta}$	3.635453	0.49010902	0.18296039	3.245802	0.45790579	0.20505185
	$\hat{\phi}$	3.256266	0.11317821	0.05965783	1.733029	0.04167597	0.04643333
100	$\hat{\delta}$	3.628916	0.29588796	0.12891568	3.193659	0.22339738	0.09365928
	$\hat{\phi}$	3.251519	0.06912407	0.05151947	1.720589	0.01831857	0.02058905
200	$\hat{\delta}$	3.579705	0.13590608	0.07970521	3.150419	0.10244596	0.05041940
	$\hat{\phi}$	3.223139	0.02919574	0.02313906	1.712680	0.00879078	0.01267982
300	$\hat{\delta}$	3.536373	0.08309930	0.03637285	3.134978	0.06239675	0.03497812
	$\hat{\phi}$	3.219773	0.01983180	0.01977281	1.705663	0.00526076	0.00566342
400	$\hat{\delta}$	3.528194	0.05809400	0.02819428	3.126003	0.04614219	0.02600261
	$\hat{\phi}$	3.208438	0.01450189	0.00843785	1.706392	0.00407558	0.00639235
500	$\hat{\delta}$	3.534524	0.04779026	0.02452407	3.125451	0.03827620	0.02545129
	$\hat{\phi}$	3.216824	0.01169161	0.00682373	1.707730	0.00328317	0.00772964
600	$\hat{\delta}$	3.523039	0.03942668	0.01954983	3.110604	0.02802522	0.01060438
	$\hat{\phi}$	3.209791	0.00976335	0.00358663	1.704034	0.00293009	0.00403422
700	$\hat{\delta}$	3.523696	0.03665965	0.01233131	3.122301	0.02572226	0.00930116
	$\hat{\phi}$	3.209870	0.00889687	0.00287570	1.702880	0.00251753	0.00287977
800	$\hat{\delta}$	3.515870	0.02973397	0.01087033	3.111488	0.02196607	0.00926814
	$\hat{\phi}$	3.206578	0.00777515	0.00257764	1.704276	0.00210844	0.00225319
900	$\hat{\delta}$	3.513368	0.02551899	0.00575817	3.110888	0.02007064	0.00801669
	$\hat{\phi}$	3.204044	0.00605281	0.00231860	1.702017	0.00192783	0.00184369
1000	$\hat{\delta}$	3.508801	0.02364411	0.00480092	3.113697	0.01543170	0.00696537
	$\hat{\phi}$	3.203020	0.00560062	0.00171976	1.705008	0.00149407	0.00120796

7. Applications

Here, we assess the flexibility and effectiveness of the NLPP-IWD by analyzing two types of real-world datasets from diverse fields. After applying the suggested distribution to these datasets, we evaluated its performance in comparison to nine other well-known probability models.

7.1. Description of the datasets

The first data set (hereafter denoted by Dataset I) contains twenty (20) observations and represents the life period of the 20 patients receiving analgesics. The Data set I is chosen from the research paper proposed by Shah et al. [18]. The values of the Dataset I are displayed as follows: 1.4, 1.1, 1.3, 1.7, 1.8, 1.9, 2.2, 1.6, 2.7, 1.7, 1.8, 1.2, 4.1, 1.5, 3, 1.4, 2.3, 1.7, 2.0, 1.6.

The second data set (hereafter denoted by Dataset II) consists of one hundred and twenty-eight (128) observations. The Dataset II represents the time in seconds between the arrival of vehicles at a specific location on the road, taken from Kumar et al. [19]. The corresponding values of the Dataset II are presented as follows: 0.2, 0.5, 0.8, 0.8, 0.8, 1.0, 1.1, 1.2, 1.2, 1.2, 1.2, 1.2, 1.3, 1.4, 1.5, 1.5, 1.6, 1.6, 1.6, 1.7, 1.8, 1.8, 1.8, 1.8, 1.8, 1.9, 1.9, 1.9, 1.9, 1.9, 1.9, 1.9, 2.0, 2.1, 2.1, 2.2, 2.3, 2.3, 2.4, 2.4, 2.5, 2.5, 2.5, 2.6, 2.6, 2.7, 2.8, 2.8, 2.9, 3.0, 3.0, 3.1, 3.2, 3.4, 3.7, 3.9, 3.9, 3.9, 4.6, 4.7, 5.0, 5.1, 5.6, 5.7, 6.0, 6.0, 6.1, 6.6, 6.9, 6.9, 7.3, 7.6, 7.9, 8.0, 8.3, 8.8, 8.8, 9.3, 9.4, 9.5, 10.1, 11.0, 11.3, 11.9, 11.9, 12.3, 12.9, 12.9, 13.0, 13.8, 14.5, 14.9, 15.3, 15.4, 15.9, 16.2, 17.6, 20.1, 20.3, 20.6, 21.4, 22.8, 23.7, 24.7, 29.7, 30.6, 31.0, 33.7, 34.1, 34.7, 36.8, 40.1, 40.2, 41.3, 42.0, 44.8, 49.8, 51.7, 55.7, 56.5, 58.1, 70.5, 72.6, 87.1, 88.6, 91.7, 119.8, 125.3.

Similarly, the third data set (hereafter denoted by Dataset III) consists of forty-four (44) observations. Dataset III represents the survival time of patients with head and neck cancer and is taken from the paper of Shanker et al. [20]. The corresponding observations of the Dataset III are presented as follows: 12.20, 23.74, 23.56, 25.87, 37, 41.35, 31.98, 47.38, 55.46, 58.36, 63.47, 68.46, 78.26, 74.47, 81.43, 84, 92, 94, 110, 112, 119, 127, 130, 133, 140, 146, 155, 159, 173, 179, 194, 195, 209, 249, 281, 319, 339, 432, 469, 519, 633, 725, 817, 1776.

For Dataset I, Dataset II, and Dataset III, some key descriptive measures are min=[1.10, 0.20, 12.20], 1st Qu=[1.475, 1.975, 67.21], median=[1.70, 5.85, 128.50], 3rd Qu=[2.05, 16.55, 219.00], mean=[1.90, 15.809, 223.48], range=[3.00, 125.10, 1763.80], variance=[0.4958, 561.5942, 93286.41], skewness=[1.7198, 2.5054, 3.3838], kurtosis=[5.9241, 9.6585, 16.5596], and max=[4.10, 125.30, 1776.0]. Likewise, for Dataset I, Dataset II, and Dataset III, some important basic plots (to display the distributional nature of the considered datasets), including the Kernel density plot, violin plot, and Box plot, are sketched in Figures 3-5. From these visualized Figures, it is indicated that all the considered data sets (i.e., Dataset I (see Figure 3), Dataset II (see Figure 4), and Dataset III (see Figure 5)) are positively skewed, and a positively skewed distribution would be a good candidate for modeling these data sets.

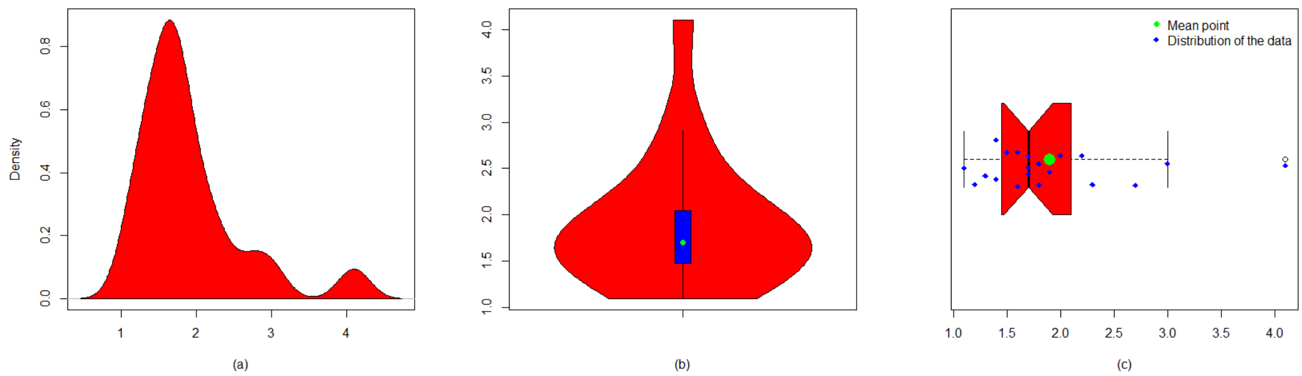

Figure 3. The Kernel density (a), Violin plot (b), and Box plot (c) for Dataset I.

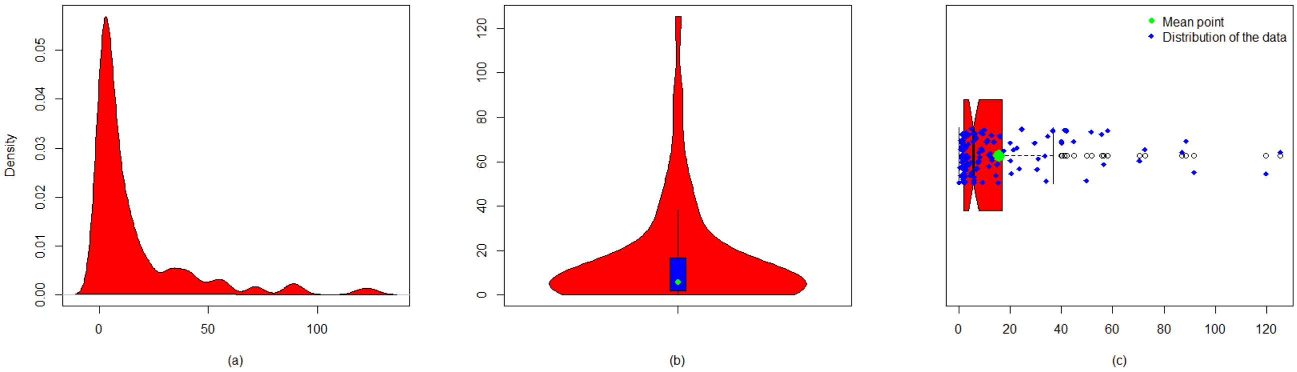

Figure 4. The Kernel density (a), Violin plot (b), and Box plot (c) for Dataset II.

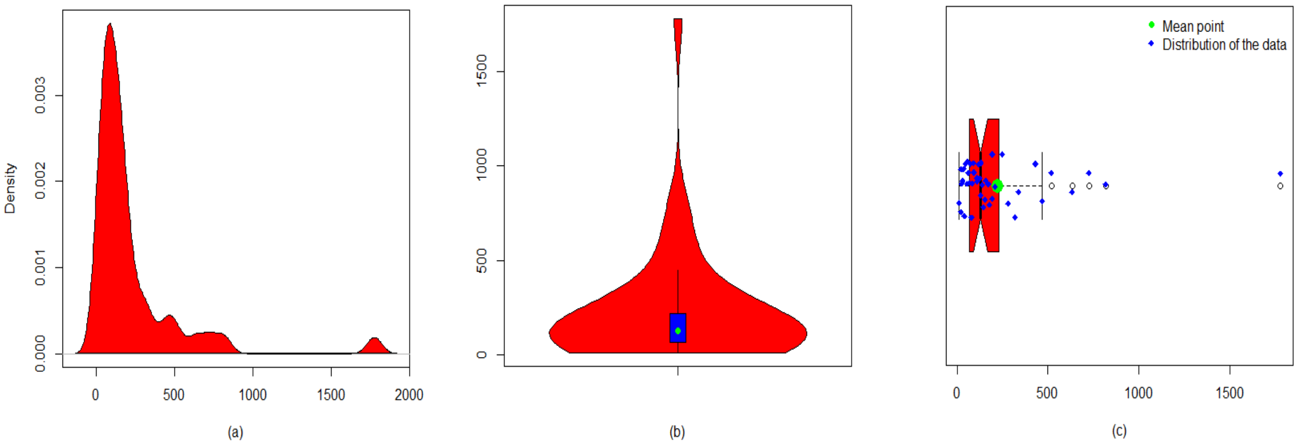

Figure 5. The Kernel density (a), Violin plot (b), and Box plot (c) for Dataset III.

7.2. Competing distributions

We apply the newly introduced NLPP-IWD to each dataset to assess its versatility and preeminence over the other ten well-known existing distributions. These competing distributions are most well-known in the literature on probability distributions. The comparison is made with the APT-W (alpha power transformation Weibull) proposed by Dey et al. [21], the new Cosine-Weibull (NC-W) developed by Ahmad et al. [12], weighted cosine-Weibull (WC-W) proposed by Odhah et al. [22], classical Weibull probability distribution introduced by Weibull [23], the Marshal Olkin Weibull (MO-W) proposed by Marshall and Olkin [24], new exponent Weibull suggested by Shah et al. [25], the NAPT-W distribution proposed by Elbatal et al. [7], the new flexible exponent power-Weibull (NFEP-W) proposed by Shah et al. [26], the novel odd type Weibull (NOT-W) proposed by Shah et al. [27], and the Gull alpha power Weibull (GAP-W) distribution proposed by the authors Ijaz et al. [28]. The SFs of these selected models are presented, respectively, by

$$S(t;\alpha,\tau)=1-\frac{\alpha^{\left(1-e^{-\delta t^{\phi}}\right)}-1}{\alpha-1}; \qquad \alpha,\delta,\phi>0, t\in\Re^{+},$$

$$S(t;\tau)=\cos\left(\frac{\pi\left(2-2^{e^{-\delta t^{\phi}}}\right)}{2}\right); \qquad \delta,\phi>0, t\in\Re^{+},$$

$$S(t;\tau)=1-\frac{e^{1-\cos\left(\frac{1-e^{-\delta t^{\phi}}}{2-e^{-\delta t^{\phi}}}\right)}-1}{e-1}; \qquad \delta,\phi>0, t\in\Re^{+},$$

$$S(t;\tau)=e^{-\delta t^{\phi}}; \qquad \delta,\phi>0, t\in\Re^{+},$$

$$S(t;\tau)=1-\frac{(1-e^{-\delta t^{\phi}})}{\left(\sigma+(1-\sigma)(1-e^{-\delta t^{\phi}})\right)}; \qquad \sigma,\delta,\phi>0, t\in\Re^{+},$$

$$S(t;\tau)=\frac{\left(e^{e^{-\delta t^{\phi}}}-1\right)}{\left(e-e^{-\delta t^{\phi}})\right)}; \qquad \delta,\phi>0, t\in\Re^{+},$$

$$S(t;\alpha,\tau)=1-\frac{\left(1-e^{-\delta t^{\phi}}\right)\alpha^{\left(1-e^{-\delta t^{\phi}}\right)}}{\alpha}; \qquad \alpha,\delta,\phi>0, t\in\Re^{+},$$

$$S(x;\alpha,\tau)=\left(e^{\alpha\left(1-e^{-\delta t^{\phi}}\right)^{2}}-e^{\alpha}\left(1-e^{-\delta t^{\phi}}\right)^{2}\right); \qquad \alpha,\delta,\phi>0, t\in\Re^{+},$$

$$S(t;\alpha,\tau)=1-\frac{(e-1)^{\alpha}\left(1-e^{-\delta t^{\phi}}\right)}{\left(e-\left(1-e^{-\delta t^{\phi}}\right)\right)^{\alpha}}; \qquad \alpha,\delta,\phi>0, t\in\Re^{+},$$

and

$$S(t;\alpha,\tau)=1-\frac{a\left(1-e^{-\delta t^{\phi}}\right)}{a^{\left(1-e^{-\delta t^{\phi}}\right)}}; \qquad \alpha,\delta,\phi>0, t\in\Re^{+}.$$

7.3. Model selection measures

This subsection presents a summary of the model selection measures that are employed to evaluate the practical performance of the NLPP-IWD and other competing distributions. The model selection measures are based on GFT (goodness-of-fit tests) and IC (information criteria). The following four measures, such as (I) Akaike IC (AIC, onward denoted by Ξ_1), (II) Bayesian IC (BIC, onward denoted by Ξ_2), (III) Consistent Akaike IC (CAIC, onward denoted by Ξ_3), and (IV) Hannan-Quinn IC (HQIC, onward denoted by Ξ_4) measures are included in IC. Similarly, the following four measures, such as (I) Kolmogorov-Smirnov (KS, indicated onward by Ξ_5) test, (II) Anderson-Darling (AD, onward indicated by Ξ_6) test, (III) Cramer von Mises (CM, onward indicated by Ξ_7) test, and (IV) their associated P-values, are included in the GFT. Furthermore, the mathematical expressions of these matrices, respectively, are presented by

$$AIC=2m-2\ell(\Upsilon),$$

$$BIC=m\log(n)-2\ell(\Upsilon),$$

$$CAIC=\frac{2mn}{m-n-1}-2\ell(\Upsilon),$$

$$HQIC=2m\log\left[\log(n)\right]-2\ell(\Upsilon),$$

$$KS = \underset{i=1,2,3\ldots n}{Max}\left(\left(\frac{i}{n}-G\left(t_{(i)}\right)\right),\left(G\left(t_{(i)}\right)-\frac{i-1}{n}\right)\right),$$

$$AD = -n-\frac{1}{n}\sum_{i=1}^{n}(2i-1)\times\left[\log\left(1-G\left(t_{(1+i-n)}\right)\right)+\log\left(G\left(t_{(i)}\right)\right)\right],$$

and

$$CM = \sum_{i=1}^{n}\left(G\left(t_{i}\right)-\frac{2i-1}{2n}\right)^{2}+\frac{1}{12n}.$$

In the above decisive instrument, the term m indicate the number of parameters, n represent the SS (sample size), and $\ell(\Upsilon)$ represent Log-LF. For each data sets, all the above measures are numerically computed by using R computer software with AdequacyModel package and BFGS algorithm. These decisive tools are widely used to determine the most suitable and optimal distribution among the fitted probability distributions. Generally, a probability model that has the lowest values of the model selection criteria and the highest P-value indicates the superior distribution for the corresponding data set. According to these evaluation measures, it is concluded that the NLPP-IWD demonstrates the lowest values across the above criteria and the highest P-value as compared to the other rival probability distributions.

7.4. Analysis of dataset I

Linked to Dataset I, the estimated parameter values along with their related standard errors (SE) for the NLPP-IWD and other competing (or rival) distributions are recorded in Table 5. The MLE method is employed to obtain these estimates. Additionally, for these estimated parameter values, the profile Log-Likelihood Functions (Log-LF) plots are sketched in Figure 6. These visualized figures clearly indicate that the corresponding estimated parameters have unique roots and maximize the Log-LF of the NLPP-IWD. Furthermore, the numerical values of the Ξ_1, Ξ_2, Ξ_3, and Ξ_4 are recorded in Table 6. Similarly, the numerical values of the Ξ_5, Ξ_6, Ξ_7 and their corresponding P-values are presented in Table 7. From Tables 6 and 7, it is numerically demonstrated that the NLPP-IWD takes the lowest values of Ξ_1, Ξ_2, Ξ_3, Ξ_4, Ξ_5, Ξ_6, Ξ_7 and the highest P-value for the considered data. Based on Dataset I, for the NLPP-IWD, the adequacy measures and P-values are Ξ_1=34.80499, Ξ_2=36.79645, Ξ_3=35.51087, Ξ_4=35.19374, Ξ_5=0.09596, Ξ_6=0.1635664, Ξ_7=0.0289606, and P-value=0.9928. In support of Ξ_1, Ξ_2, Ξ_3, Ξ_4, Ξ_5, Ξ_6, and Ξ_7, the second best (or superior) distribution is the NOT-W distribution. Likewise, in support of the P-value, the second superior probability model is the MO-W distribution because its P-value is the second highest. Furthermore, linked to Dataset I, the graphical illustrations (or representations), such as the PDF, CDF, PP, and QQ plots of the NLPP-IWD, are illustrated in Figure 7. From Figure 7, it is also graphically demonstrated that the NLPP-IWD model provides a better fit to the concerned data set (i.e., Dataset I) compared to the other competing probability distributions.

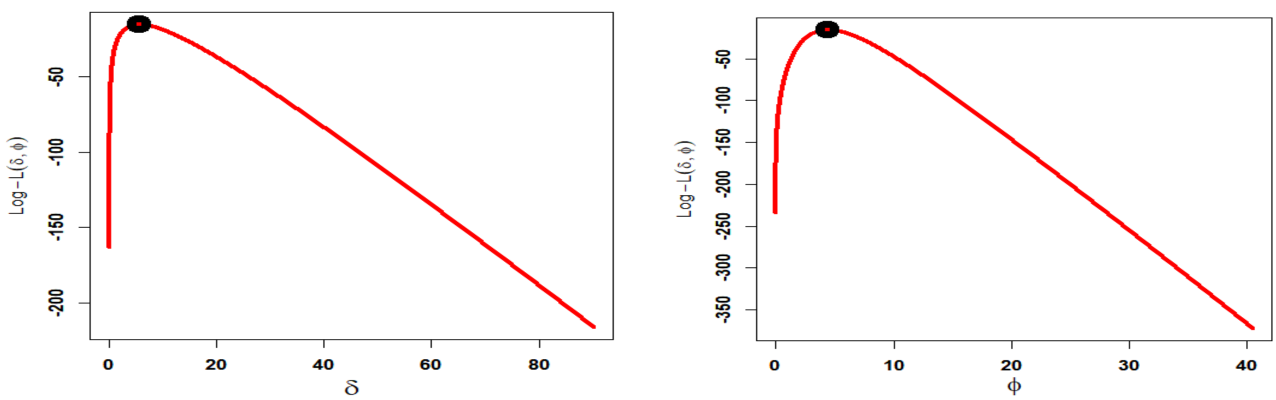

Figure 6: The log-likelihood profile of the $\hat{\delta}_{MLE}$, and $\hat{\phi}_{MLE}$ of the NLPP-IWD for Data set I.

Table 5. For Dataset I, MLEs with SE.

Distributions	Parameters	SE	Parameters	SE	Parameters	SE
NLPP-IWD(δ,ϕ)	5.455384	1.9727223	4.389370	0.7475912	–	–
APT-W(α,δ,ϕ)	0.0158580	0.0336694	0.0207352	0.0150870	3.6200613	0.5587130
NC-W(δ,ϕ)	0.1990451	0.0663244	2.4172847	0.3533914	–	–
WC-W(δ,ϕ)	0.2072990	0.0717835	2.4128480	0.3567617	–	–
Weibull(δ,ϕ)	0.1215765	0.0562406	2.7869457	0.4272109	–	
MO-W (σ,δ,ϕ)	0.0479274	0.0356381	0.0037108	0.0024442	4.4051448	0.5948351
NE-W(δ,ϕ)	0.0460279	0.0229355	3.3233764	0.4791494	–	–
NAPT-W(α,δ,ϕ)	53.6526320	77.2953050	0.7345892	0.2384752	1.6611311	0.2985984
NFEP-W(α,δ,ϕ)	0.8220111	0.22183980	0.2541606	0.0828198	2.2147346	0.3429236
NOT-W(α,δ,ϕ)	80.9874046	140.230613	2.4623955	1.5319043	0.9337885	0.3716460
GAP-W(α,δ,ϕ)	2.22833459	0.51915900	0.04523612	0.02494305	3.26722914	0.49178586

Table 6. The values of Ξ_1, Ξ_2, Ξ_3, and Ξ_4 of the fitted probability models for Dataset I.

Distributions	Ξ_1	Ξ_2	Ξ_3	Ξ_4
NLPP-IWD	34.80499	36.79645	35.51087	35.19374
APT-W	43.41718	46.40437	44.91718	44.00031
NC-W	41.04621	43.03768	41.75209	41.43497
WC-W	41.81054	43.80201	42.51643	42.19930
Weibull	45.17281	47.16427	45.87869	45.56156
MO-W	40.81321	43.80041	42.31321	41.39634
NE-W	42.93560	44.92706	43.64148	43.32435
NAPT-W	43.20095	46.18815	44.70095	43.78409
NFEP-W	42.94296	45.93016	44.44296	43.52609
NOT-W	38.48855	41.47574	39.98855	39.07168
GAP-W	44.85181	47.83901	46.35181	45.43494

Table 7. The values of Ξ_5 Ξ_6, Ξ_7, and P-values of the fitted distributions for Dataset I.

Distributions	Ξ_5	Ξ_6	Ξ_7	P-Values
NLPP-IWD	0.09596	0.1635664	0.0289606	0.9928
APT-W	0.15792	0.7784422	0.1324223	0.7008
NC- W	0.17956	0.7477086	0.1255368	0.5392
WC- W	0.18322	0.8166551	0.1375724	0.5130
Weibull	0.18495	1.0928700	0.1857121	0.5007
MO- W	0.14609	0.4689762	0.0782901	0.8527

NE- W	0.18129	0.9042441	0.1521853	0.5267
NAPT-W	0.16321	0.7472262	0.1262447	0.6611
NFEP-W	0.16531	0.7367722	0.1248414	0.6452
NOT-W	0.14085	0.3189593	0.0542618	0.8224
GAP-W	0.17162	0.9046673	0.1536728	0.5978

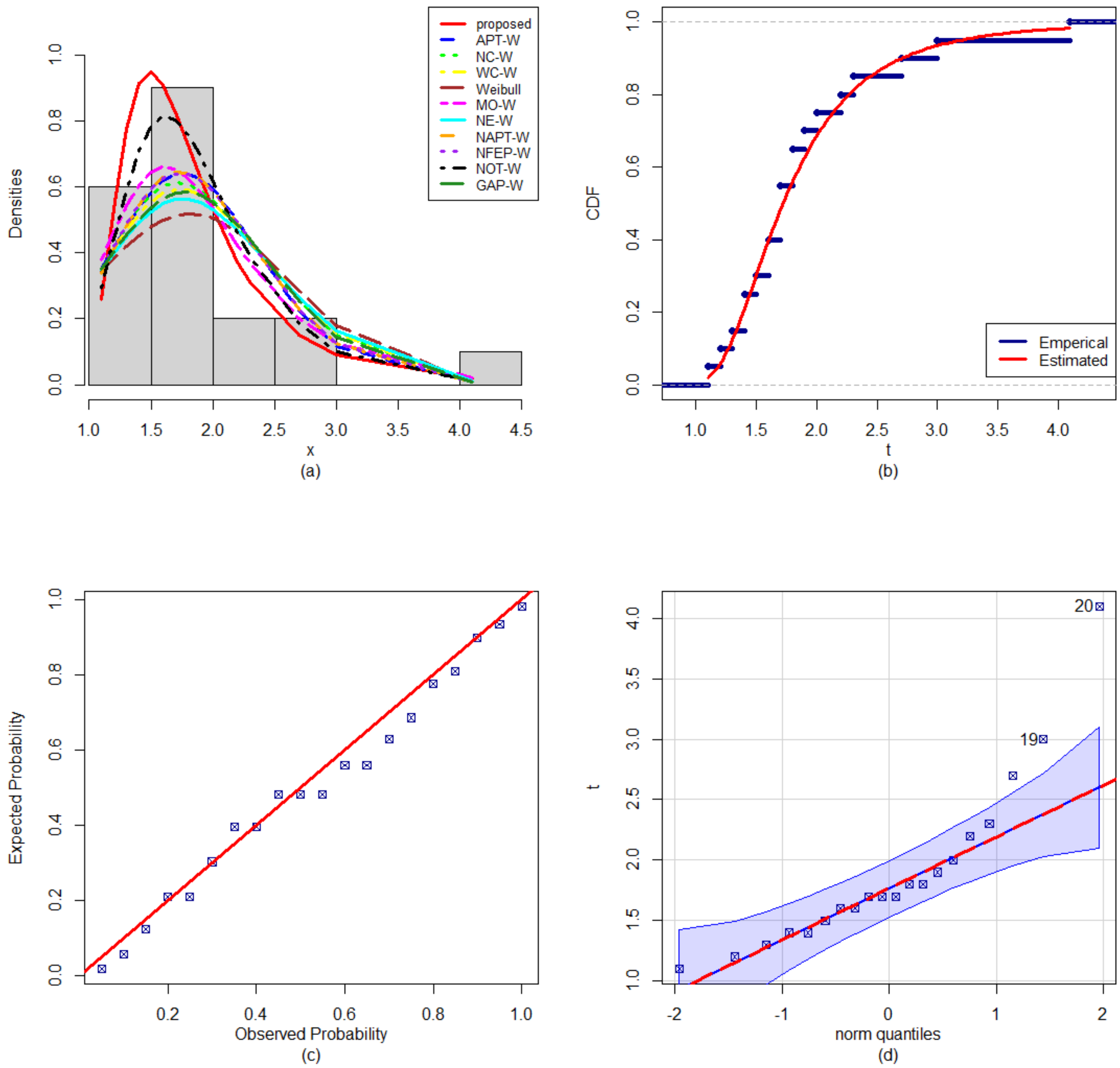

Figure 7. The graphical illustration of the (a) estimated PDF, (b) estimated CDF, (c) estimated SF, and (d) Q-Q plot of the NLPP-IWD for Dataset I.

7.5. Analysis of dataset II

Similarly, linked to Dataset II, the estimated model parameter values along with their related SE for the NLPP-IWD and other competing distributions are recorded in Table 8. The MLE method is employed to obtain these estimates. Additionally, for these estimated parameter values, the profile Log-LF plots are sketched in Figure 8. These figures demonstrate that the estimators of the NLPP-IWD (the estimated parameter values) have unique roots and also maximize the Log-LF of the NLPP-

IWD. Furthermore, the information criteria (IC) such as Ξ_1, Ξ_2, Ξ_3, and Ξ_4 are documented in Table 9. Similarly, the numerical values of the GFT statistics measures, such as Ξ_5 Ξ_6, Ξ_7 along with their corresponding P-values for all models under comparison are presented in Table 10. From Tables 9 and 10, it is numerically demonstrated (or verified) that the NLPP-IWD distribution is also the optimum probability distribution for the considered data set. The newly introduced NLPP-IWD also takes the lowest values of IC (i.e., Ξ_1, Ξ_2, Ξ_3, and Ξ_4) and GFT (i.e., Ξ_5, Ξ_6, and Ξ_7), and the highest P-value for the second data set. Based on Dataset II, for the NLPP-IWD distribution, the adequacy measures and P-values are Ξ_1 =924.0384, Ξ_2 =929.7425, Ξ_3=924.1344, Ξ_4 =926.3560, Ξ_5=0.06407, Ξ_6=1.003333, Ξ_7 =0.152616, and P-value=0.6695. In support of Ξ_1, Ξ_3, Ξ_5, Ξ_6, Ξ_7, and the P-value, the second best (or superior) distribution is the MO-W probability distribution. Similarly, in support of Ξ_2 and Ξ_4 the second superior probability model is the NC-W model because its Ξ_2 and Ξ_4 values are minimum. Furthermore, linked to Dataset II, the graphical (or visual) representations, such as the PDF, CDF, PP, and QQ plots of the NLPP-IWD, are illustrated in Figure 9. From Figure 9, it is also graphically demonstrated that the NLPP-IWD model provides a close fit to the concerned data set (i.e., Dataset II) compared to the other competing probability distributions.

Table 8. For Dataset II, MLEs with SE.

Distributions	**Parameters**	**SE**	**Parameters**	**SE**	**Parameters**	**SE**
NLPP-IWD (δ,ϕ)	2.2249570	0.23381779	0.8919311	0.05687018	_	_
APT-W(α,δ,ϕ)	0.08238703	0.08083913	0.04947435	0.01877895	0.88730294	0.05971378
NC-W(δ,ϕ)	0.26885872	0.03255689	0.6065565	0.03737141	_	_
WC-W(δ,ϕ)	0.27351625	0.03475686	0.6122164	0.03807244	_	_
Weibull(δ,ϕ)	0.14877851	0.0267172	0.7462223	0.0488899	_	_
MO-W (σ,δ,ϕ)	0.07478915	0.04059976	0.00886125	0.00515755	1.14343681	0.08367920
NE-W(δ,ϕ)	0.06368568	0.01214159	0.87002497	0.05477198	_	_
NAPT-W (α,δ,ϕ)	0.52662136	0.10316658	0.07349616	0.02074697	0.83753281	0.05476733
NFEP-W(α,δ,ϕ)	0.64204032	0.21809426	0.3626549	0.05394329	0.5514305	0.03513563
NOT-W(α,δ,ϕ)	-0.99105106	0.41494294	0.09017755	0.02476407	0.80462842	0.05323055
GAP-W(α,δ,ϕ)	1.90126785	0.37178896	0.07335929	0.02067676	0.83772540	0.05474546

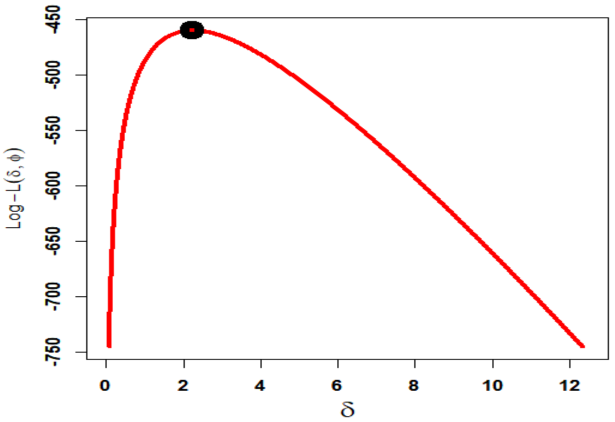

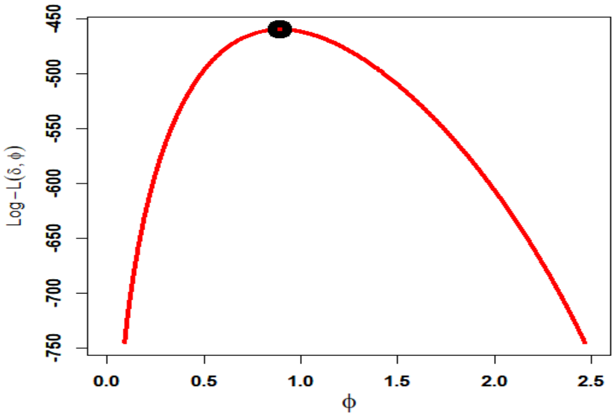

Figure 8. Profile log-likelihood plots for $\hat{\delta}_{MLE}$ and $\hat{\phi}_{MLE}$ of the NLPP-IWD for Dataset II.

Table 9. The values of Ξ_1, Ξ_2, Ξ_3, and Ξ_4 of the fitted models for Dataset II.

Distributions	Ξ_1	Ξ_2	Ξ_3	Ξ_4
NLPP-IWD	924.0384	929.7425	924.1344	926.3560
APT-W	937.7630	946.3191	937.9566	941.2394
NC- W	929.6481	935.3521	929.7441	931.9657
WC- W	931.8038	937.5078	931.8998	934.1213
Weibull	943.4808	943.3848	943.4808	945.7024
MO- W	929.0036	937.5597	929.1972	932.4800
NE-W	936.2622	941.9663	936.3582	938.5798
NAPT-W	940.0746	948.6307	940.2681	943.5510
NFEP-W	934.3341	942.8901	934.5276	937.8104
NOT-W	941.8872	950.4432	942.0807	945.3635
GAP-W	940.0746	948.6307	940.2681	943.5510

Table 10. The values of Ξ_5 Ξ_6, Ξ_7, and P-values of the fitted distributions for Dataset II.

Distributions	Ξ_5	Ξ_6	Ξ_7	P-Values
NLPP-IWD	0.06407	1.003333	0.152616	0.6695
APT-W	0.11273	2.640458	0.4316863	0.0773
NC- W	0.11564	2.241017	0.3662949	0.06521
WC- W	0.11849	2.406589	0.3932636	0.05498
Weibull	0.11626,	3.205793	0.5259759	0.06284
MO- W	0.10135	1.983291	0.3271201	0.14422
NE-W	0.11376	2.696639	0.4408201	0.07283
NAPT-W	0.11416	2.819558	0.4611651	0.07115
NFEP-W	0.11562	2.408579	0.3935326	0.06529
NOT-W	0.11471	2.948795	0.4826662	0.06893
GAP-W	0.11424	2.819728	0.4611922	0.07079

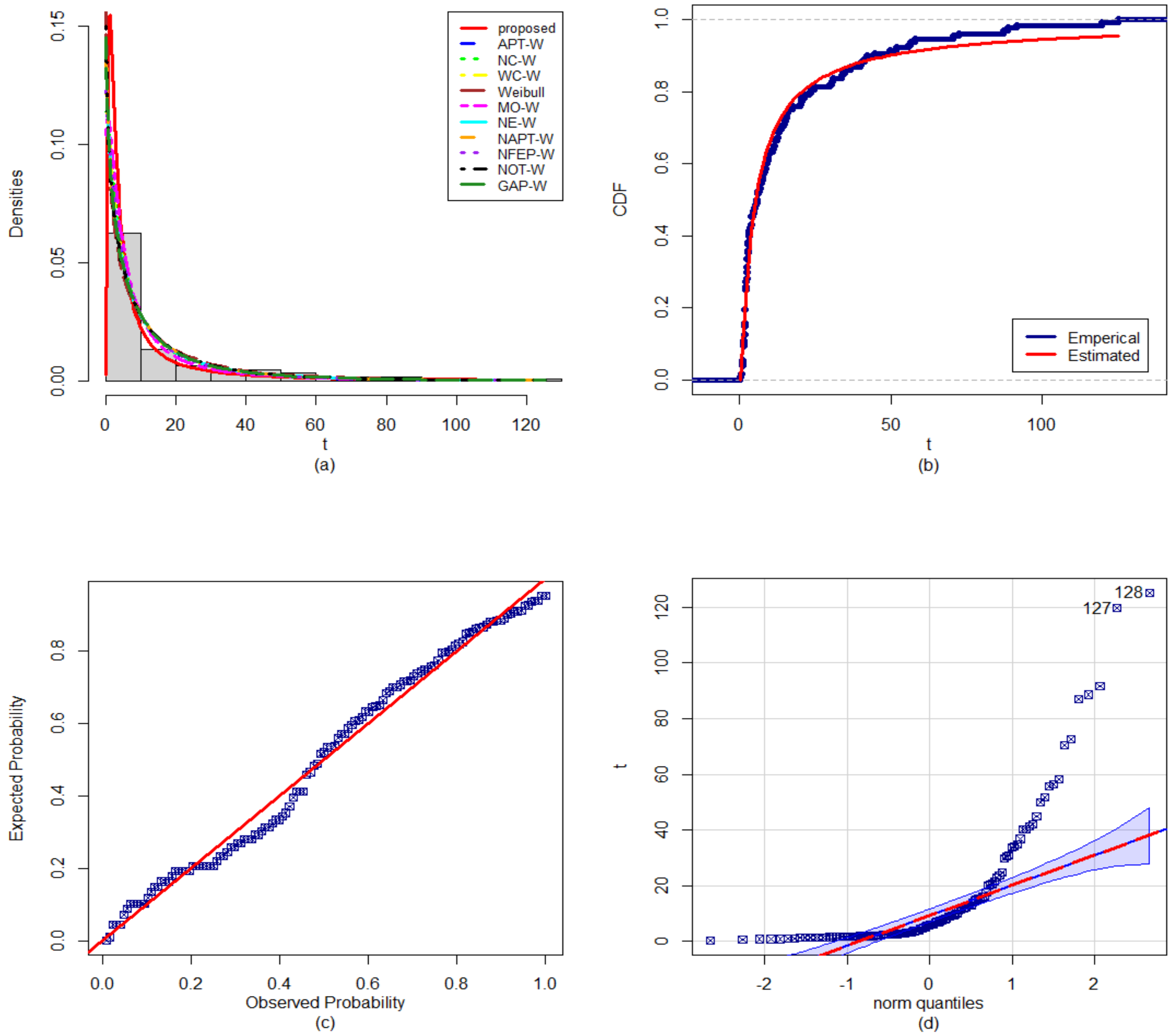

Figure 9. The graphical illustration of (a) estimated PDF, (b) estimated CDF, (c) estimated SF, and (d) Q-Q plot of the NLPP-IWD for Dataset II.

7.6. Analysis of dataset III

Likewise, linked to Dataset III, the estimated model parameter values along with their related SE (standard errors) for the NLPP-IWD and other competing distributions are recorded in Table 11. The MLE method is employed to obtain these estimates. Similarly, for these estimated parameter values, the profile Log-LF plots are sketched in Figure 10. These figures demonstrate that the estimators of the NLPP-IWD have unique roots and also maximize the Log-LF of the NLPP-IWD. Furthermore, the IC such as Ξ_1, Ξ_2, Ξ_3, and Ξ_4 are presented in Table 12, while the numerical values of the GFT statistics measures, such as Ξ_5 Ξ_6, Ξ_7 along with their corresponding P-values of the fitted distributions are presented in Table 13. From Tables 12 and 13, it is numerically demonstrated that the newly introduced NLPP-IWD distribution is an optimum probability distribution for the considered data set, as it also has the lowest values of IC and GFT, and the highest P-value.

Based on Dataset III, for the NLPP-IWD distribution, the adequacy measures and P-values are Ξ_1=561.3070, Ξ_2=565.8754, Ξ_3=562.5997, Ξ_4=563.6304, Ξ_5=0.090609, Ξ_6=0.4074342, Ξ_7=0.0657794, and P-value=0.8511. In support of Ξ_1, Ξ_2, Ξ_3, and Ξ_4 the second superior distribution is the WC-W distribution. Similarly, in support of Ξ_5, Ξ_6, Ξ_7, and P-value, the second superior probability model is the NAPT-W model because its Ξ_5, Ξ_6, and Ξ_7 values are minimum and higher P-value. Furthermore, linked to Dataset III, the graphical (or visual) representations, such as the PDF, CDF, PP, and QQ plots of the NLPP-IWD, are illustrated in Figure 11. From Figure 11, it is also graphically observed that the NLPP-IWD model provides a better fit to the third (i.e., Dataset III) compared to the other competing probability distributions.

Table 11. For Dataset II, MLEs with SE.

Distributions	**Parameters**	**SE**	**Parameters**	**SE**	**Parameters**	**SE**
NLPP-IWD (δ,ϕ)	95.695363	47.3286664	1.1162180	0.1196996	_	_
APT-W(α,δ,ϕ)	0.2450304	0.28574304	0.00326450	0.00113197	0.9927009	0.0597341
NC-W(δ,ϕ)	0.0187569	0.00825014	0.78090553	0.07803986	_	_
WC-W(δ,ϕ)	0.0187277	0.00845830	0.78797092	0.07890537	_	_
Weibull(δ,ϕ)	0.0067712	0.00321090	0.93131153	0.07942888	_	_
MO-W (σ,δ,ϕ)	0.5075243	0.21052035	0.00303242	0.00090366	1.0011885	0.0539074
NE-W(δ,ϕ)	0.0020126	0.000165237	1.05444359	0.03268741	_	_
NAPT-W(α,δ,ϕ)	65.511827	74.80369407	0.1622548	0.07357954	0.5157339	0.0721952
NFEP-W(α,δ,ϕ)	0.7953193	0.24017504	0.02917051	0.01247805	0.7143021	0.0786072
NOT-W(α,δ,ϕ)	1.3097549	0.708047100	0.00320375	0.00086886	0.9094594	0.1195507
GAP-W(α,δ,ϕ)	0.0023792	0.002376302	0.21971348	0.06986458	0.4795036	0.0540656

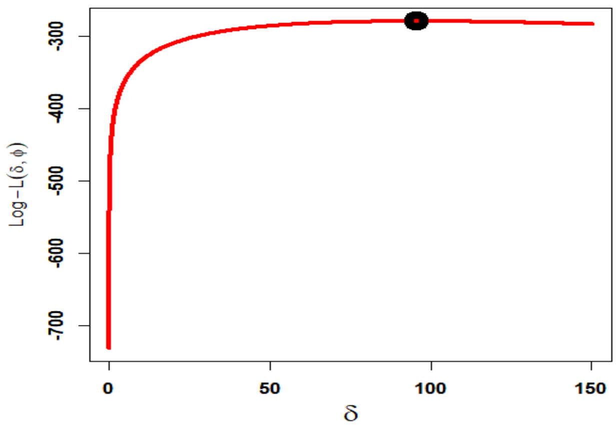

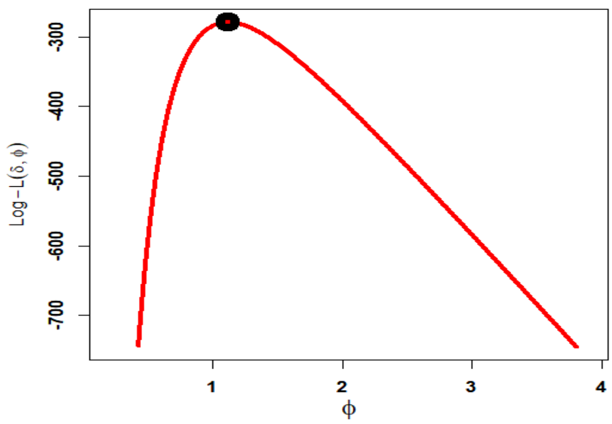

Figure 10. Profile log-likelihood plots for $\hat{\delta}_{MLE}$ and $\hat{\phi}_{MLE}$ of the NLPP-IWD for Dataset III.

Table 12. The values of Ξ_1, Ξ_2, Ξ_3, and Ξ_4 of the fitted models for Dataset III.

Distributions	Ξ_1	Ξ_2	Ξ_3	Ξ_4
NLPP-IWD	561.3070	565.8754	562.5997	563.6304
APT-W	567.7712	573.1238	568.3712	569.7562
NC- W	564.9928	566.5612	564.2855	565.3161
WC- W	563.8449	566.4133	563.1376	564.1683
Weibull	567.6941	571.2625	567.9868	569.0175
MO- W	568.2084	573.5616	568.8084	570.1934
NE-W	564.8069	568.3743	565.0986	566.1293
NAPT-W	564.5487	569.8926	565.1498	566.5258
NFEP-W	564.1153	569.4678	564.7153	565.1003
NOT-W	566.7386	567.4832	566.0894	567.2394
GAP-W	563.8822	568.5547	563.8022	565.1872

Table 13. The values of Ξ_5 Ξ_6, Ξ_7, and P-values of the fitted distributions for Dataset III.

Distributions	Ξ_5	Ξ_6	Ξ_7	P-Values
NLPP-IWD	0.090609	0.4074342	0.0657794	0.8511
APT-W	0.105510	0.5538716	0.0933868	0.6723
NC- W	0.102554	0.4831426	0.0740322	0.7059
WC- W	0.109843	0.4591399	0.0775534	0.6236
Weibull	0.126129	0.8142793	0.1398368	0.4494
MO- W	0.112559	0.5618123	0.0949219	0.5933
NE-W	0.107869	0.5356683	0.0900657	0.6459
NAPT-W	0.096975	0.4448119	0.0654892	0.8047
NFEP-W	0.097132	0.4598813	0.0686631	0.7965
NOT-W	0.1089495	0.4954683	0.0850568	0.7859
GAP-W	0.0979721	0.4475422	0.06986719	0.7972

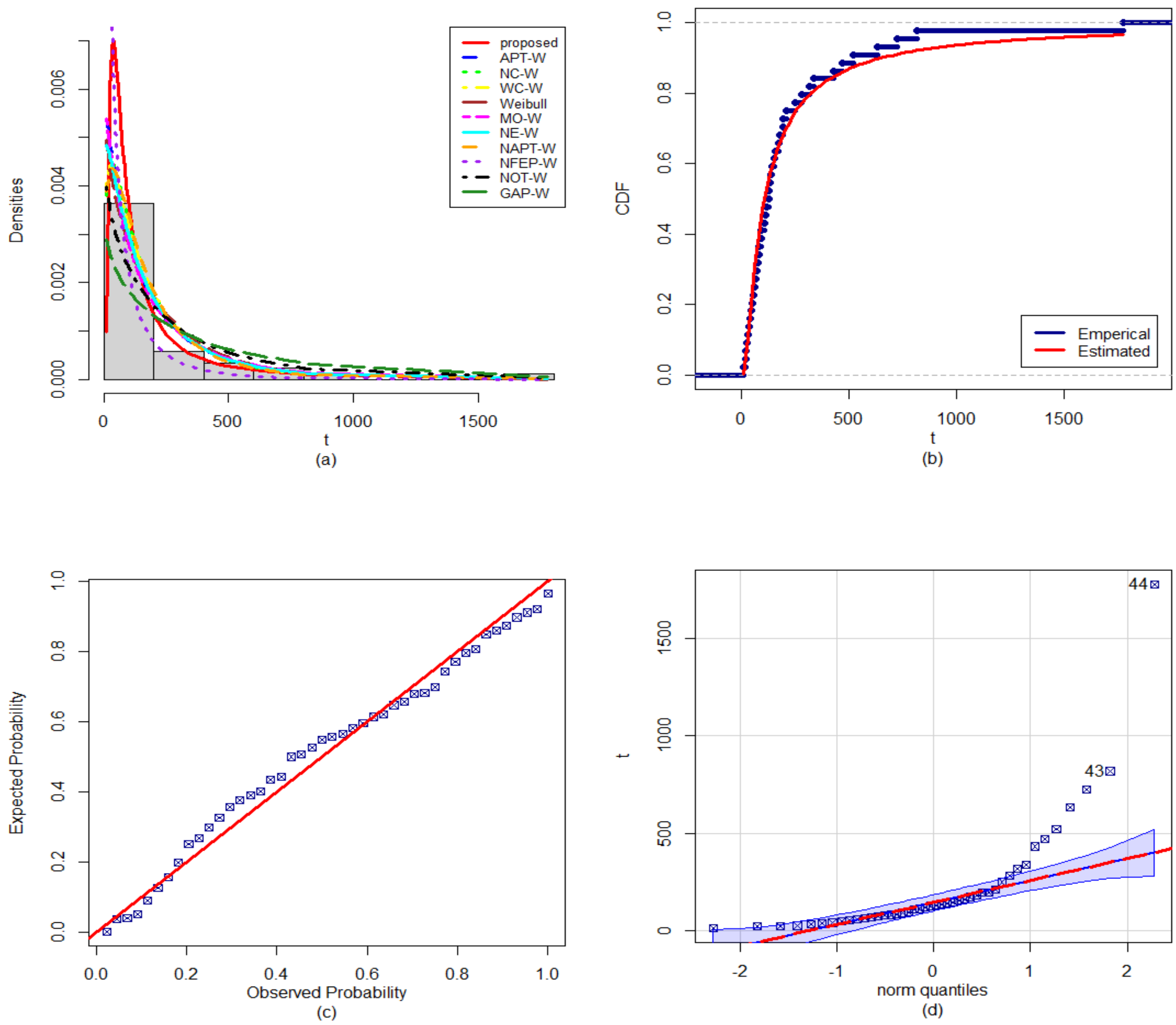

Figure 11. The graphical illustration of (a) estimated PDF, (b) estimated CDF, (c) estimated SF, and (d) Q-Q plot of the NLPP-IWD for Dataset III.

8. Concluding Remarks

In the present article, we have proposed a novel flexible family of distributions called the New Logarithmic Pie Power-G family of probability distributions. This newly proposed approach can recommend more new distributions without adding extra shape or scale parameters. Furthermore, we have used the traditional Inverse Weibull distribution as a base member of the newly introduced approach and recommended a versatile model called the New Logarithmic Pie Power Inverse Weibull distribution (NLPP-IWD). The CDF, SF, PDF, and HF of the NLPP-IWD are investigated graphically, and flexibility is observed from these illustrations. Some statistical (or distributional) properties of the NLPP-IWD are also investigated. Similarly, the most popular MLE approach is applied for estimating the model parameters of the newly developed NLPP-IWD distribution. MCSS is conducted to verify the recital of the MLE method. Based on the MCSS process, it is concluded that the Biases and MSEs are decreased as the corresponding sample size increases and the MLE estimates converge toward the true parameter values. Finally, we applied the NLPP-IWD to two real data sets (the data sets are taken from the medical and engineering fields) and evaluated its performance by comparing it with nine well-known distributions. Our numerical and graphical findings confirm the dominance of the proposed model. We believe that this newly presented improvement in the field of distribution theory and its special cases can be useful in a variety of domains, including medical science, survival analysis, and reliability engineering. It may also encourage the researchers to generate more versatile probability models in the future.

Authors' Contributions

Conceptualization, Z.S., Z.A., and G.S.R.; Methodology, Z.S.; Software, Z.S., Z.A, and G.S.R; Formal Analysis, Z.S., Z.A., Z.A., and G.S.R.; Investigation, Z.S., F.K., C.K.O., and S.K.K.; Data Curation, Z.S., Z.A., F.K., C.K.O., G.S.R., and S.K.K.; Validation, F.K., C.K.O., G.S.R., and S.K.K.; Resources, C.K.O., G.S.R., and S.K.K.; Writing –Original Draft Preparation, Z.S., and Z.A.; Writing –Review & Editing, Z.A., F.K., C.K.O., G.S.R., and S.K.K.; Visualization, Z.S., Z.A., and G.S.R.; Supervision, Z.S., Z.A., and G.S.R.; Project Administration, C.K.O., and G.S.R..

Data Availability Statement

This article included all the data that is generated or evaluated during the present investigation.

Conflicts of Interest

The authors declare no conflict of interest.

Funding

This research received no external funding.

Use of Generative-AI tools declaration

The authors declare they have not used Artificial Intelligence (AI) tools in the creation of this article.

References

1. Alsadat, N., Ahmad, A., Jallal, M., Gemeay, A. M., Meraou, M. A., Hussam, E., Elmetwally , E. M. & Hossain, M. M. (2023). The novel Kumaraswamy power Frechet distribution with data analysis related to diverse scientific areas. *Alexandria engineering journal*, *70*, 651-664.
2. Almalki, S. J., & Yuan, J. (2013). A new modified Weibull distribution. *Reliability Engineering & System Safety*, *111*, 164-170.
3. Mudholkar, G. S., & Srivastava, D. K. (1993). Exponentiated Weibull family for analyzing bathtub failure-rate data. *IEEE transactions on reliability*, *42*(2), 299-302.
4. Kumar, D., Singh, U., & Singh, S. K. (2015). A new distribution using sine function-its application to bladder cancer patients data. *Journal of Statistics Applications & Probability*, *4*(3), 417.
5. Maurya, S. K., Kaushik, A., Singh, R. K., Singh, S. K., & Singh, U. (2016). A new method of proposing distribution and its application to real data. *Imperial Journal of Interdisciplinary Research*, *2*(6), 1331-1338.
6. Mahdavi, A., & Kundu, D. (2017). A new method for generating distributions with an application to exponential distribution. *Communications in Statistics-Theory and Methods*, *46*(13), 6543-6557.
7. Elbatal, I., Ahmad, Z., Elgarhy, M., & Almarashi, A. M. (2018). A new alpha power transformed family of distributions: properties and applications to the Weibull model. *Journal of Nonlinear Science and Applications*, *12*(1), 1-20.
8. Mahmood, Z., Chesneau, C., & Tahir, M. H. (2019). A new sine-G family of distributions: properties and applications. *Bull. Comput. Appl. Math.*, *7*(1), 53-81.
9. Muhammad, M., Bantan, R. A., Liu, L., Chesneau, C., Tahir, M. H., Jamal, F., & Elgarhy, M. (2021). A new extended cosine—G distributions for lifetime studies. *Mathematics*, *9*(21), 2758.
10. Alizadeh, M., MirMostafee, S. M. T. K., Ortega, E. M., Ramires, T. G., & Cordeiro, G. M. (2017). The odd log-logistic logarithmic generated family of distributions with applications in different areas. *Journal of Statistical Distributions and Applications*, *4*(1), 6.

11. Lone, M. A., & Jan, T. R. (2023). A new Pi-exponentiated method for constructing distributions with an application to Weibull distribution. *Reliability: Theory & Applications*, *18*(1 (72)), 94-109.
12. Ahmad, A., Jallal, M., & Mubarak, S. A. (2023). New cosine-generator with an example of Weibull distribution: Simulation and application related to banking sector. *Reliability: Theory & Applications*, *18*(1 (72)), 133-145.
13. Sapkota, L. P., Kumar, P., Kumar, V., Tashkandy, Y. A., Bakr, M. E., Balogun, O. S., Getachew, T. M. & Gemeay, A. M. (2024). Sine π-power odd-G family of distributions with applications. *Scientific Reports*, *14*(1), 19481.
14. Kavya, P., & Manoharan, M. (2021). Some parsimonious models for lifetimes and applications. *Journal of Statistical Computation and Simulation*, *91*(18), 3693-3708.
15. Lone, M. A., Dar, I. H., & Jan, T. R. (2022). A new method for generating distributions with an application to Weibull distribution. *Reliability: Theory & Applications*, *17*(1 (67)), 223-239.
16. Elgarhy, M., Metwally, D. S., Ragab, I. E., Bashiru, S. O., Semary, H. E., & Gemeay, A. M. (2025). The DUS-transformed generalized linear failure rate distribution: Properties, estimation, and applications. *Scientific African*, *29*, e02891.
17. Bashiru, S. O., Abdalla, G. S. S., Ragab, I. E., Elbatal, I., Gemeay, A. M., & Elgarhy, M. (2025). Type II Half-Logistic Rayleigh Weibull distribution with statistical inference and applications. *Scientific African*, e02927.
18. Shah, Z., Khan, D. M., Khan, Z., Faiz, N., Hussain, S., Anwar, A., Ahmad, T. & Kim, K. I. (2023). A new generalized logarithmic–X family of distributions with biomedical data analysis. *Applied Sciences*, *13*(6), 3668.
19. Kumar, P., Sapkota, L. P., & Kumar, V. (2023). π-Power Half Logistic-G family: Applications to medical and traffic data. *Reliability: Theory & Applications*, *18*(4 (76)), 575-590.
20. Shanker, R., Shukla, K. K., Shanker, R., & Tekie, A. L. (2016). On modeling of lifetime data using two-parameter gamma and Weibull distributions. *Biometrics & Biostatistics International journal*, *4*(5), 1-6.
21. Dey, S., Sharma, V. K., & Mesfioui, M. (2017). A new extension of Weibull distribution with application to lifetime data. *Annals of Data Science*, *4*(1), 31-61.
22. Odhah, O. H., Alshanbari, H. M., Ahmad, Z., & Rao, G. S. (2023). A weighted cosine-G family of distributions: Properties and illustration using time-to-event data. *Axioms*, *12*(9), 849.
23. Weibull, W. (1951). A statistical distribution function of wide applicability. *Journal of applied mechanics*.
24. Marshall, A. W., & Olkin, I. (1997). A new method for adding a parameter to a family of distributions with application to the exponential and Weibull families. *Biometrika*, *84*(3), 641-652.
25. Shah, Z., Ali, A., Hamraz, M., Khan, D. M., Khan, Z., El-Morshedy, M., Al-Bossly, A. & Almaspoor, Z. (2022). A New Member of T-X Family with Applications in Different Sectors. *Journal of Mathematics*, *2022*(1), 1453451.
26. Shah, Z., Khan, D. M., Khan, I., Ahmad, B., Jeridi, M., & Al-Marzouki, S. (2024). A novel flexible exponent power-X family of distributions with applications to COVID-19 mortality rate in Mexico and Canada. Scientific Reports, 14(1), 8992.
27. Shah, Z., Almetwally, E. M., Khan, D. M., & Jamal, F. (2025). A novel odd Type-X family of distributions: Model, theory, and applications to medical, insurance, and engineering data sets. Journal of Radiation Research and Applied Sciences, 18(2), 101451.
28. Ijaz, M., Asim, S. M., Alamgir, Farooq, M., Khan, S. A., & Manzoor, S. (2020). A Gull Alpha Power Weibull distribution with applications to real and simulated data. Plos one, 15(6), e0233080.

© 2026 by the authors. **Disclaimer / Publisher's Note:** The views, opinions, and data presented in all published content are solely those of the individual authors and contributors. They do not necessarily reflect the positions of Sphinx Scientific Press (SSP) or its editorial team. SSP and the editors disclaim any responsibility for harm or damage to individuals or property that may result from the use of any information, methods, instructions, or products mentioned in the content.